NAVORD REPORT 6164

STAT

FAST FIELD EFFECT AND PHOTORESPONSE STUDIES ON LEAD SULFIDE PHOTOCONDUCTORS

15 MAY 1958

U. S. NAVAL ORDNANCE LABORATORY
WHITE OAK, MARYLAND

NAVORD Report 6164

FAST FIELD EFFECT AND PHOTORESPONSE STUDIES ON LEAD SULFIDE PHOTOCONDUCTORS

STAT

ABSTRACT: Concurrent studies of field effect and photoconductivity in thin-film lead-sulfide photoconductors have yielded a better understanding of the mechanism of photoconductivity involved. Two problems were of particular concern: (a) the validity of the assumptions of the majority carrier model of photoconductivity[1], and (b) the role of the electronic traps probed by field effect in the photoconductive process.

Experimental data from chemically deposited lead sulfide films confirm the existence of electronic traps on the surface and/or in the space charge region and demonstrate for the first time the identity of the field effect and photoresponse time constants. A beat frequency bridge technique applied to the fast field effect measurements permitted heretofore impossible accuracy, particularly if the samples are of high impedance. The majority carrier model was extended, by including explicitly the time for charge transfer into and out of the majority carrier traps, to describe the field effect data. Analysis of the data shows the rate of transfer of charge into the majority carrier traps to be the limiting process. Density and capture-cross-section of the majority carrier traps were estimated.

Principle conclusions are that (a) the assumptions of the majority carrier model are valid and (b) the electronic traps probed by field effect are a representative sample of those which cause photoconductivity. The latter conclusion means that field effect measurements will be a useful tool for further classification of the mechanisms for photoconductivity in thin-film photoconductors of the lead salt type.

U. S. NAVAL ORDNANCE LABORATORY
WHITE OAK, MARYLAND

This report describes an experimental and theoretical study of the fundamental mechanism of photoconductivity in lead-sulfide thin-film photoconductors. The study is a part of a research program at the Naval Ordnance Laboratory for the purpose of better understanding the photoconductive process in lead salt photoconductors. Experimental data consist of a series of concurrent photoresponse and field effect measurements. The principal achievement of the experiment was the substantial confirmation of a majority carrier model [1] previously conceived in this Laboratory for the description of photoconductivity in the lead salt type thin-film photodetector. Theoretical contributions include (a) the extension of the majority carrier model to include explicitly electronic trapping on the surface and in the space charge region and to describe field effect, and (b) an analysis of experimental results which provides for the first time estimates of values for such fundamental properties as effective capture cross section and densities of the traps which cause photoconductivity in the lead sulphide films.

TABLE OF CONTENTS

STAT

ILLUSTRATIONS

I. INTRODUCTION

A. Objectives

The overall problem is to identify the fundamental mechanism of photoconductivity in thin-film infrared detectors of the lead salt type. The specific objectives are to determine: (a) the role of electronic states probed by field effect in the photoconductive process and (b) the validity of the majority carrier model[1] for describing photoconductivity in the films.

B. Summary of Previous Investigations

1. Engineering and Scientific Interest: Thin film photodetectors, sometimes called photoconductors or photocells, are of considerable interest to the military and to industry. Their remarkable sensitivity, fast response time, small size, convenient geometry, light weight, and high gain are all desirable properties. Therefore, thin-film detectors are now produced in large quantity for use in a wide variety of scientific, military, and industrial instruments. There is also considerable scientific interest in the properties of these detectors. Extensive bibliographies in review papers 2, 3, 4, 5 show the quantity of experimental data and number of theories concerning the physical, electrical, and optical properties of the films. However, in spite of the intense academic and industrial interest, particularly during the past decade, the identification of the fundamental mechanism

for the observed photoconductivity in the lead salt type of film remains one of the tantalizing problems of photoconductor theory[2] and the films are still fabricated by empirically developed processes which are not completely understood. The identification and understanding of this mechanism has obvious practical as well as scientific value, e.g. novel and improved photocells can then be engineered with properties required for specific applications.

2. Physical Properties and Fabrication Techniques: Physical properties and fabrication techniques are particularly important when considering the mechanism for photoconductivity. Films are a composite of microscopic crystallites formed by either vacuum evaporation or chemical deposition of the lead-salt to a thickness of about one micron on a glass substrate. The chemically deposited films are sensitized, i.e. rendered photosensitive, during deposition. This sensitization may be optimized after deposition by baking the film in air or oxygen. Vacuum evaporated films are sensitized by exposure to oxygen either during or after the condensation. According to X-ray and electron microscope observations,[6] the crystallites have overall dimensions of the order 0.1 micron and are separated by intercrystalline barriers with thicknesses of the order of 10 A°, (see Fig. 1). The individual crystallites are lead salts, while the intercrystalline barriers are an oxide of the lead salts or of lead. The microscopic dimensions afford a relatively large surface to volume ratio, thus emphasizing the role which surface states might play in the photoconductive process.

3. Photoconductivity in the Lead-Salt Type Detectors: Although photoconductivity was discovered in selenium by W. Smith in 1873,[8] the marked photoconductivity of the lead-salt

type materials was not discovered until 1917 when Case[9] studied oxygen treated thallous sulfide which he named thallofide. According to Rose,[3] photoconductivity was not interpreted in terms of the lifetime of a free carrier and the capture cross section of a bound state for free carriers before about 1945.[4] The excellent review papers by Rittner,[2] Moss,[4] Smith,[5] and Petritz and Humphrey[10] reveal the numerous theories and models proposed between 1945 and 1957 for describing photoconductivity in these films. The experimental effort was correspondingly large. Research on the electrical and optical properties of the lead-salt type films will now be summarized by considering the fundamental processes involved in a manner similar to that of Petritz and Humphrey.[10,11]

The principal processes of photoconductivity are the generation and the recombination of free carriers. The generation of free carriers by the absorption of photons was shown to be a main band transition by the agreement of the thermal energy gap[12] with optical transition energy determined from the long wavelength limit of photoconductivity.[13] Since the optical transitions are main band ones, they occur in the crystallites rather than in the barriers.[1] Having established the process of generation, a significant remaining problem is to establish the process of recombination. The prior research on this problem will be classified and discussed under one of three categories depending on the carrier lifetime of importance. The first category is the intrinsic carrier model in which recombination is either by recombination centers or directly between bands. Both the number and the lifetime of free electrons and holes are approximately equal, a condition presumably achieved by the sensitization process. The early theory of von Hipple and Rittner,[14] which is typical of this category, proposes photoresponse to be characteristic

of a uniform intrinsic semiconductor produced by detailed balancing of n and p-type impurities. A basic deficiency of this model is the failure to predict the measured small ratio of film to single crystal mobilities.[2] The second category is the minority carrier model in which photoconductivity depends on a long minority carrier lifetime. The film is visualized as a composite of microscopic n-p-n junctions. In a theory for this model developed by Slater,[15] barrier modulation plays an important role. Barrier modulation theory has been successful in predicting certain electrical and photoconductive properties of PbS films.[16] The third category is the majority carrier model in which photoconductivity results from the predominance of the majority carrier. The free minority carrier created by the photon is thought to be trapped, leaving the corresponding majority carrier free to conduct. Petritz[1] developed a theory for this model which has been successful in predicting noise,[17] responsitivity, sensitivity,[18] Hall coefficient, and resistivity[19] measurements on PbS films.

In identifying the photoconductive processes in the lead-salt type films, history has demonstrated that while success in describing the experimental data at hand is necessary, it does not lead to a unique theory. Rose[20] concludes that a unique deduction of the mechanism of photoconductivity by the study of a particular substance is hardly possible, and Slater[15] points out that more than one mechanism might be present simultaneously in PbS. In spite of these inherent difficulties, certain recent experiments furnish strong evidence as to the appropriate model. Humphrey and Scanlon[21] reported studies on evaporated PbS films which showed that although other oxidizing elements formed acceptor sites in the film, only oxygen produced photoconductivity at room temperature. If either the intrinsic or minority carrier

models were applicable, any acceptor element should produce photoconductivity. A plausible interpretation is that oxygen was the only acceptor element which formed the minority carrier required by the majority carrier model. Also, Woods[19] concluded from his measurements of resistivity and Hall coefficient of illuminated chemically-deposited PbS films, that photoconductivity is entirely due to the increase in the number of carriers and that barrier modulation does not occur.

The theory[1] for the majority carrier model does not specify where the minority carriers are trapped. The mean free path of the minority carriers is sufficiently long relative to the dimensions of the crystallite[2] to permit trapping in either the surface or bulk states. Estimates by Petritz[22] show that the density of the surface traps, i.e. bound electronic states on the surface of the crystallite, is adequate to account for the observed photoconductive time constants. If the trapping cross section of the surface states for the minority carriers is sufficiently large, the surface instead of the bulk traps could predominate in the photoconductive process.

4. Electronic Surface States: Although there is little in the literature concerning the electronic surface states of PbS, there is considerable relevant information on other materials in the review article by Kingston[23] and in Semiconductor Surface Physics.[24] The concept of surface states was first proposed by Tamm,[25] who in 1928 showed theoretically that an abrupt discontinuity of the crystal at the surface allows an energy level within the forbidden energy gap of the crystal. In 1939 Shockley[26] showed theoretically that pairs or bands of energy levels exist on the surface of semiconductors (he considered diamond) and all metals. In 1947 Bardeen[27] showed that electronic states on the surface of semi-

conductors could, under favorable conditions, control the electrical properties of the material. Numerous experiments[23,24] since the advent of the transistor have confirmed Bardeen's postulate as applied to germanium and silicon. As a result of these experiments, an electronic energy level model of the semiconductor surface of the type shown in Fig. 2 is now generally accepted.

In the studies on germanium and silicon surfaces, the bound states have been classed as "slow" or "fast" depending on the time required for net transfer of charge between the surface states and the bulk. Slow states have time constants in the range from milliseconds to minutes and are visualized as resulting from acceptor or donor sites located either on or/and in the high resistance oxide layer which coats the semiconductor crystal. Estimates based on experimental data indicate that the densities of slow surface states are in the range of 10^{12} to 10^{14} cm^2. These states are strongly affected by ambient atmosphere. The fast states have time constants of the order of microseconds and are believed to be located on or near the oxide-semiconductor interface. They are often called interface states. These states may result from several sources such as the abrupt discontinuity in crystal structure, crystal defects, and foreign acceptor or donor atoms or molecules at the crystal surface. Fast states seem to be relatively insensitive to ambients and their densities are estimated to be in the range of 10^{11} to 10^{12} cm^2.

Recent experiments have shown that electronic surface states exist on PbS films in much the same manner as they exist on germanium and silicon. Zemel[28] reports slow states with time constants of the order of several minutes. Rezewoski and Sosnowski[29] found that electronic states exist on the surface of PbS films which can affect the

electrical conductance. Sorrows[30] reported fast field effect studies on a PbS film which not only confirmed the findings of Rezewoski and Sosnowski, but showed that the field effect time constant and the photoresponse time constants were approximately equal. Methods of sensitizing, particularly in the case of the vacuum evaporated films, suggest that surface states play an important role in establishing both the electrical and photoconductive properties. Resistivity and thermoelectric power measurements show that films formed by vacuum evaporation are "n" type prior to sensitization. Upon sensitization by exposure to oxygen the films are "p" type. Conceivably, the change in electrical and optical properties is caused by surface states formed during the exposure to oxygen. The manner in which the surface states could change the electrical properties of the film is explained by use of Fig. 2. The presence of oxygen on the crystallite surfaces creates accepter sites which trap electrons. The electrostatic field from these trapped charges causes the indicated bending of the electron energy level bands near the surface. In fact if sufficient charge is trapped, an inversion layer is created, i.e. the region near the surface is changed from "n" to "p" type. The space charge regions in PbS crystallites have not been studied experimentally; however, theoretical calculations indicate that the region extends about 0.07 micron into the crystallite.[2] The space charge region of the small crystallites of the PbS films could control the electrical properties of the film. In the case of chemically deposited films of the type used in this study, considerable sensitization occurs during the deposition process.[4] The crystallites which compose the film are then thought to be "p" type with an accumulation layer at the surface.[31] This concept is illustrated in the energy level diagrams (Figs. 3 and 4) for a PbS photoconductive film.

Trapping in fast surface states on germanium has been studied by field effect measurements. This measurement probes only those states which are on the surface or within the space charge layer of the surface. According to the energy level diagram for the PbS photoconductive film surface shown in Fig. 4, the states which exist on the surface crystallites of the film are a representative sample of those on the surfaces of all the crystallites which compose the film (Fig. 1). Field effect measurements should then provide information concerning the nature of the surface state and space charge region traps of the crystallites.

C. Approach

In view of (a) the success of the majority carrier model[1] in describing both the electrical and photoconductive properties of the lead-salt films and (b) the suggestion[11] that electronic surface states might be the traps required by the majority carrier model, it was decided to further investigate the basic assumptions of the majority carrier model and the role of electronic surface states. To do this a series of concurrent field effect and photoresponse measurements were made on PbS films. Two fundamental differences in field effect and photoresponse are pertinent in this study. First, only majority carriers are induced into the film in field effect measurements, whereas hole-electron pairs are created in the film by the photons in the photoresponse measurements. Second, only the surface and space charge region traps are probed in field effect, whereas surface, space charge, and bulk traps affect the photoresponse.

The main components for the study are shown in Fig. 5. In field effect measurements, a voltage on the field effect plate causes an

external electric field transverse to the film surface. This field is superimposed on that from the surface state charge. The external field then affects the electrical properties of the space charge layer in much the same manner as do the trapped surface charges. The field effect measurements can provide the time constant τ_t associated with the charge transfer between the space charge region and the surface traps, the fraction α of the total external field lines terminating on immobile charges at quasi-equilibrium, and the mobility μ_f of the excess charges induced into the film. In measuring photoresponse, the change in electrical conductance caused by incident light pulses is determined as a function of either time or light pulse repetition rate. The measurement yields τ_r , the photoresponse time constant. Transient and steady state field effect and photoresponse were measured as a function of background illumination, film surface condition, and sensitivity of the film.

PbS films were chosen for the study because (a) they are typical of the lead-salt type photodetector, (b) the art of fabrication is far more advanced than for other members of this class of photodetector, and (c) there is already a considerable accumulation of information concerning the electrical and photoconductive properties of PbS in both the film and bulk form which aids in interpretation of experimental data.

II. EXPERIMENT

A. Apparatus

1. Film Samples: With the exception of one sample furnished by the Naval Ordnance Laboratory, samples (similar to that shown as an insert in Fig. 5) were furnished by Eastman Kodak Company. The films were formed by chemical deposition on a glass substrate and some of the samples had the free surface coated with varnish. The Eastman Kodak Company films were sensitized when received. A film furnished by NOL had purposely not been sensitized and the surface was uncoated.

2. Sample Holder: The holder, Figs. 6a and b, was made from teflon stock. When assembled with the sample properly mounted, one surface of the film surface was parallel to the solid brass field-effect plate. The other surface was exposed to both the controlled background illumination and to the pulsed light. Most of the measurements were made with the field effect plate on one side of the film and the light sources on the opposite side. A perforated field-effect plate, fabricated by pressing a fine mesh wire into a heated transparent sheet, permitted a series of measurements with the field effect plate and the light sources on the same side of the film.

3. Sample Housing: The housing shown in Figs. 7a and b was made of heavy brass stock to afford a large heat capacity and could be sealed off from the atmosphere. This design was chosen

to prevent rapid fluctuations in both film temperature and ambient during measurements. The housing consisted of two sections separated by a fine mesh screen; the sample holder was firmly mounted in the bottom section, and the top section contained the background illumination and the pulsed light sources. A standard incadescent lamp (6-8 volt Mazda 82) was used (Fig5) and its intensity was selected by adjusting the dc voltage across the lamp terminals. The source for the light pulses was a 0.4 watt neon glow tube (NE-2). Electromagnetic coupling between the circuitry associated with the sample and that associated with the light sources was prevented by use of the fine mesh screen.

4. Balanced Bridge: The commercial titles of the principal electrical instruments used in the balanced bridge shown in Fig. 8 are as follows:

Function	Commercial Title
Stabilized Voltage Supply	Lee Model R-10
Voltage Pulse Generator	Tektronix Type 105
Differential Amplifier	Tektronix Type 122
Cathode Ray Oscilloscope	Tektronix Type 512
Micro Amp Meter	Weston Model 625

5. Beat-Frequency Bridge: The commercial titles of the principal electrical instruments used in the beat-frequency bridge shown in Fig. 9 are as follows:

Function	Commercial Title
Sq. Wave Voltage Gen.	Tektronix 105
Audio Signal Gen., Freq. b	(Hewlett Packard
Audio Signal Gen., Freq. f	(Model 205 AG
Vacuum Tube Voltmeter, V_b	General Radio 1800 A
Vacuum Tube Voltmeter, V_f	Ballentine 300
Wave Analyzer	General Radio 736A or H.P. 300A

B. Procedure

1. Transient Field Effect and Photoresponse Measurements: Transient changes in film conductance caused by both square wave field effect voltages and pulsed light signals were observed with the balanced bridge shown in Fig. 8. The square wave voltages used to drive the field effect plate and the neon glow tube were purposely made asymmetrical in time in order to establish the relative signs of the respective bridge responses. The initial step for field effect measurement was to balance the bridge with no film current I_s and a square wave voltage V_f applied to the field effect plate. This was done by alternately adjusting R_1 or R_2 and the trimmer capacitors (labeled 1.5 - 7.5$\mu\mu$fd) until the differential output voltage across the film terminals was a minimum. When the bridge was balanced and a current was in the film, the field induced transient conductance change ΔG caused a transient voltage ΔV_o across the film terminals. ΔV_o was amplified by the differential amplifier and displayed on the cathode ray oscilloscope. ΔV_o and ΔG are related as follows (derivation in Appendix A).

$$\Delta G = \frac{-\Delta V_o (R_1 + R_2 + R)}{I_s R^2 (R_1 + R_2)} , \qquad (1)$$

where R is the film resistance. Equation 1 is valid for photoresponse as well as field effect measurements. It is not necessary to balance the bridge for the photoresponse measurements. Since ΔG is a linear function of ΔV_o, the field effect and photoresponse time constants τ_f and τ_r respectively were estimated directly from the oscilloscope patterns.

2. Steady State Field Effect and Photoresponse Measurements: Steady state ac field effect and photoresponse were both measured on

the beat-frequency bridge shown in Fig. 9. The bridge was biased with a sinusoidal voltage V_b of frequency b and then balanced by alternately adjusting R and C until the wave analyzer tuned to b indicated a voltage minimum. Application of either a sinusoidal field effect voltage V_f at frequency f or a pulsed light at frequency f caused a resistance modulation ΔR at frequency f which beat with the bias voltage. The wave analyzer measured the beat frequency voltage V_w when tuned to either f+b or f-b, where w = f+b or f-b. In order to compare readily the field effect measurements on the various films studied, a normalized factor F_f, the fractional change in film resistance per field-effect volt at frequency f, was calculated for each measurement from the following equation:

$$F_f = \frac{\Delta R}{R V_f} = \frac{\sqrt{2}\, L_w V_w}{V_f V_b} . \qquad (2)$$

In photoresponse measurements, the fractional change in film resistance for a pulsed-light of given intensity was calculated from

$$\frac{\Delta R}{R} = \frac{L_w V_w}{V_b} . \qquad (3)$$

Equations 2 and 3 are derived in Appendix 2; V_w, V_f and V_b are rms values. The loading of the film resistance by the bridge and wave analyzer circuits is accounted for by the factor L_w and had to be determined for each film and for each selected background illumination intensity by an experimental technique described in Appendix 2. Because of its frequency dispersion, see Fig. 10, the value of L_w was chosen in each measurement for the frequency corresponding to V_w.

The selected background illumination intensity and bridge bias frequency were held

constant while both the field effect and photo-response were measured at a number of selected frequencies covering the range from 20 to 15,000 cps. The response F_f and $\Delta R/R$ of each frequency run were plotted on log-log paper and compared directly with the corresponding universal curves of Fig. 11. From this comparison, α, τ_f, and τ_D were obtained directly; μ_f was calculated from the experimental data.

C. Discussion of Measurement Methods

1. Balanced Bridge: Although the balanced bridge method has been widely used in surface state studies for both transient and steady state field effect measurements, the method is not entirely satisfactory for quantitative field effect measurements. The inherent difficulty is that a small response voltage must be measured in the presence of a large capacitively induced voltage at the same frequency or frequencies. In this particular experiment, the induced voltage was of the order of 125 volts and the response voltages were only a few millivolts. This large ratio of voltages necessitates a very precise balance. In spite of the care taken in mounting the sample securely, in the prevention of thermal and ambient changes, and in wiring the bridge circuit for minimum unbalanced stray capacitance and lead inductance; the balance was both tedious to achieve and subject to small but disconcerting drifts. The large resistance of the films and the lack of common mode range of the commercially available differential amplifier also contributed to the inherent difficulties of the measurement method. A differential amplifier with increased common mode range could have been constructed using already established techniques, but at the sacrifice of the high frequency amplification necessary to measure the field effect transients.

In the transient measurements, the magnitude of the resistance of the bridge arms (R_1 and R_2) was relatively small, of the order of 10K ohms or less, to permit charging of the condenser formed by the field-effect plate and film in less than a microsecond. This relatively short charging time was necessary in order to avoid masking field-effect transient responses, the time constants of which were as short as 100 microseconds. The condenser charging time was that required for the charge to flow through the parallel resistance of R_1 and R_2. The relatively small resistance in the bridge arms reduced the bridge sensitivity considerably below optimum.

The balanced bridge is also often used in steady-state ac field-effect measurements. All of the information contained in the transient response can be obtained from a measurement of steady-state response versus field-effect frequency. To obtain the information, response must be measured at each of a number of frequencies covering the frequency band of interest. Several such frequency runs were made. The balancing at each frequency was found tedious and the small higher harmonics of the field effect frequency source were annoying.

Both transient and steady state photo-response measurements can be made with the balanced bridge setup without balancing the bridge. These measurements are thus simple and reliable.

2. Beat-Frequency Bridge: The beat-frequency bridge, which was applied to field-effect measurements for the first time in this study, is well suited for quantitative steady state ac field-effect measurements. This bridge circumvents the basic difficulty of balanced bridges by measuring the field effect response voltage at a frequency different from the applied field effect or bias voltages.

The beat-frequency bridge operation is based on the field-effect modulation of the film resistance which beats or mixes with the bias voltage to produce sum and difference frequency voltages. There is no inherent need for bridge balancing. However, in this experiment, the bridge was sufficiently balanced to prevent the bias voltage from saturating the wave analyzer. The degree of balance required was easy to achieve and maintain. Small drifts off balance, which were disastrous in the balanced bridge measurements, caused negligible difficulty in the beat-frequency bridge. The principal requirements in the beat-frequency bridge measurements were that the field effect and bias frequencies be sufficiently stable to permit the sum or difference frequencies to remain within the pass band of the wave analyzer, and that the harmonic content of the field effect and bias voltages be sufficiently low to permit accurate measurement of these voltages with vacuum tube voltmeters. These requirements were not stringent. The ease of operation of the beat-frequency bridge is important; however, its principal virtue is the precise measurement of small field effect or photoresponse voltages.

D. Experimental Data

1. Transient Field Effect and Photoresponse Data: A large number of oscilloscope patterns of field effect and photoresponse were observed using the balanced bridge. Figure 12 is typical of the oscilloscope patterns of the transient response to a square wave field effect voltage. Figure 13 indicates the sign and time relation between transient field effect, transient photoresponse, and driving voltage. A negative deflection in the oscilloscope pattern indicates an increase in film conductance. Both the photoresponse time constant τ_p and the field effect time

constant τ_f were estimated from oscilloscope patterns for selected intensities of background illumination. The qualitative correspondence of τ_p and τ_f is shown in Fig. 14.

A number of exploratory type experiments were made using the balanced bridge. Those experiments, which contribute to the general understanding of fast surface states but are not relevant to the objectives of this study, are discussed in Appendix 4.

2. Steady State Field Effect and Photoresponse Data: The experimental data are presented for the most part in pairs of figures which present field effect and photoresponse measurements for a given surface condition and selected intensities of background illumination. The circles represent the experimental data and the solid line the universal curve which best fits the data. Figures 15 and 16 are the data for Eastman Kodak Company sample 1-B which had an uncoated surface. The field effect plate faced the uncoated surface of the film. Figures 17 and 18 are data of a film, EK Co. sample 1-A, which was of the same type as sample 1-B except for a coating on the free surface of the film. The electric field was induced through the coating. Figures 19, 20 and 21 are concerned with EK Co. sample 16, an uncoated film: in Fig. 19, the field effect plate faces the free side of the film surface; in Fig. 20, the electric field is induced through the glass substrate; and Fig. 21 is the photoresponse data. Figure 22 is the field effect response on a film, NOL 5-11-9, purposely made to be approximately 20 times less sensitive than the above films. Figure 23 compares the field effect on different types of surface and degree of sensitization.

3. Field Effect Mobility Product: The mobility product $(1+B_f)\mu_f$ was calculated from Eq.(76) for several samples. A typical set of

results for sample EK Co. 1-B as a function of background illumination is

Lamp Voltage	$(1+Bf)\mu_f$
0	4.0 cm^2/volt-second
1.5	4.4 " " "
2.5	3.0 " " "

The product is approximately 4 cm^2/volt-second with no definite trend as a function of background illumination.

4. Summary of Experimental Data: In the transient measurements, a negative square wave field effect voltage caused an instantaneous increase followed by an exponential decrease in film conductance. The decrease was a fraction α of the initial increase. When the negative field effect voltage was removed, the conductance decreased by the same increment as the initial increase and then increased exponentially with time to the equilibrium value. The time constants associated with the exponential increase and decrease of conductance were equal within experimental error and were both a function of background illumination.

In the photoresponse measurements, upon exposure of the film to a light pulse of constant intensity, the conductance increased exponentially to an equilibrium value. When the light pulse was removed, the conductance decreased exponentially with time to the original equilibrium value. Time constants for increase and decrease in conductance were approximately equal and were a function of background illumination intensity. The qualitative data indicate a correlation of field effect and photoresponse time constants as a function of background illumination (See Fig. 14).

Steady state ac field effect and photoresponse measurements with the beat-frequency bridge were a quantitative verification of the qualitative results of the transient measurements. The field effect response was a maximum at high frequency and decreased at low frequencies to a fraction $(1 - \alpha)$ of the maximum (See Fig. 24). Photoresponse was maximum at low frequencies and decreased at high frequencies. The concurrent field effect and photoresponse measurements showed that α, τ_f and τ_p were inversely dependent on background illumination intensity. There was a one-to-one correlation between τ_f and τ_p as a function of background illumination intensity. α was a function of the side of the film from which the field was induced, but τ_f was not. τ_p was independent of the side of the film from which the pulsed light was incident. α was a function of the surface conditions. An insensitive film showed a negligible value of α. A comparison of the experimental data with the theoretical universal curves indicates single effective time constants τ_f and τ_p for both field effect and photoresponse respectively. The mobility product $(1+Bf)\mu_f$ for field effect was found to be approximately equal to the mobility μ_H as determined by Hall effect measurements.[19]

III. THEORY

A. Empirical Equations Developed By RC Circuit Analogies

1. General: In the initial stages of the study reported herein, the empirical equations developed by RC circuit analogies were quite useful in describing and analyzing the experimental data. Later, these equations served as a guide in developing the theory. Because of the success of the empirical equations in describing the experimental data, any models or theories for photoconductivity or field effect in PbS must give the same equations.

2. Description of Experimental Field Effect: The overall appearance of the oscilloscope patterns of the transient field effect response ΔV_o (see Figs. 12 and 13), was similar to the transient voltage response of the RC circuit shown in Fig. 25. For this circuit the transient voltage response V_r to a step function input voltage V_i is

$$V_r = V_i \left(\frac{R_b}{R_a + R_b} + \frac{R_a}{R_a + R_b} e^{-\frac{t}{\tau}} \right), \qquad (4)$$

where τ is the RC time constant:

$$\tau = \frac{R_a R_b}{R_a + R_b} C . \qquad (5)$$

The similarity of the field effect and circuit responses leads to the following empirical equation for the voltage ΔV_o across the film terminals in response to a step function field-effect voltage V_f:

$$\Delta V_o = G_{ft} V_f \left[(1-\alpha) + \alpha e^{-\frac{t}{\tau_f}} \right] . \qquad (6)$$

The parameters G_{ft}, α, and τ_f are uniquely determined by a single observation of the transient field effect response to a step function field effect voltage. G_{ft} is the ratio $\Delta V_o / V_f$ at the start of the field effect pulse, α is the fractional decrease in response from t=0 to quasi-equilibrium and is analogous to $Ra/(Ra+R_b)$, and τ_f is the time constant of the exponential decay and is analogous to τ. α and τ_f are determined solely by the properties of the film. G_{ft} is determined by the properties of the bridge and the film to field effect plate capacity, as well as the properties of the film.

The RC circuit steady state response V_r to a sinusoidal input voltage V_i of angular frequency ω is

$$V_r = V_i \frac{\left[\left(\frac{R_b}{R_a + R_b} + \tau^2 \omega^2 \right)^2 + \left(\frac{R_a \omega \tau}{R_a + R_b} \right)^2 \right]^{\frac{1}{2}}}{1 + \omega^2 \tau^2} . \qquad (7)$$

The corresponding field effect response V_w is then

$$V_w = V_f G_{fs} \frac{\left[\left(1 - \alpha + \tau_f^2 \omega^2 \right)^2 + (\alpha \omega \tau_f)^2 \right]^{\frac{1}{2}}}{1 + \omega^2 \tau_f^2} . \qquad (8)$$

Referring to Fig. 24, α is the fractional decrease in response from maximum to minimum and τ_f can be calculated from $\omega_s\tau_f=1$, where ω_s is the angular frequency at which the response is $(1-\alpha+\frac{1}{2}\alpha^2)^{\frac{1}{2}}$ of maximum. Therefore α and τ_f can be determined from the relative steady state ac field effect response as a function of frequency while an absolute calibration is needed to obtain G_{fs}. The calculations of universal curves, Fig. 11, for relative field effect were based on Eq. (8), in which

$$\text{relative response} = \frac{\left[\left(1-\alpha+\omega^2\tau_f^2\right)^2+\alpha^2\omega^2\tau_f^2\right]^{\frac{1}{2}}}{1+\omega^2\tau_f^2}. \quad (9)$$

Since the frequency dependent part of Eq. (8) becomes unity and V_w is maximum at high frequency

$$G_{fs} = \frac{V_{w(max)}}{V_f}. \quad (10)$$

The fractional change in resistance per field effect volt as obtained from Eqs. (2) and (8) is

$$F_f = \Delta R/RV_f = \frac{\sqrt{2}\,L_w G_{fs}}{V_b}\,\frac{\left[\left(1-\alpha+\omega^2\tau_f^2\right)^2+\alpha^2\omega^2\tau_f^2\right]^{\frac{1}{2}}}{1+\omega^2\tau_f^2}. \quad (11)$$

3. Description of Photoresponse: The transient response to a pulsed light signal (see Fig. 13) was similar to that of the RC circuit shown in Fig. 26. The transient response V_r to a step function input voltage

V_i for this RC circuit is

$$V_r = V_i\,\frac{R_a}{R_a+R_b}\left(1-e^{-\frac{t}{\tau}}\right), \quad (12)$$

where the RC time constant τ is

$$\tau = \frac{R_a R_b}{R_a+R_b}\,C. \quad (13)$$

Using the RC analogy, the response ΔV_o to a step function light pulse is

$$\Delta V_o = g\,G_{pt}\left(1-e^{-\frac{t}{\tau_p}}\right), \quad (14)$$

where g is the rate at which majority carriers are created in the film when the light is on, G_{pt} is a proportionality constant involving both film and balanced bridge properties, and τ_p is the photoresponse time constant. The steady state response at a frequency w=(f±b) is

$$V_w = g\,G_{ps}/\left(1+\omega^2\tau_p^2\right)^{\frac{1}{2}}, \quad (15)$$

G_{ps} is the steady state proportionality constant. τ_p, the parameter of primary interest in this study, can be calculated from the equation $\omega_o\tau_p=1$ where ω_o is the angular frequency at which the response is $1/\sqrt{2}$ of maximum. The universal curve for photoresponse, the dotted line in Fig. 11, was calculated using the frequency dependent term of Eq. (15), i.e.

$$\text{relative response} = \frac{1}{(1+\omega^2\tau_p^2)^{\frac{1}{2}}}. \qquad (16)$$

B. Theoretical Equations Based On Majority Carrier Model

1. Statement of Problem: As stated previously, the majority carrier model has been developed and applied to the calculation of the electrical and photoconductive properties of lead salt type films.[1] The objective here is to extend the model to describe the field effect by explicitly including the electronic surface states. Later the theoretical equations obtained from the extension will be compared with the experimental data, i.e. the equations developed from RC analogies. Certain concepts of Petritz' paper are restated as background material for extending the model, particularly those pertinent to the interpretation of the experimental data. The procedure is to develop the equations for the macroscopic conductance and resistance of the film from a consideration of the microscopic properties of the crystallites and intercrystalline barriers. The ideas and equations developed are then used both in the description of photoconductance and in the extension of the majority carrier model to describe field effect.

2. Film Conductance and Resistance: The microscopic semiconductor crystallites which compose the film have a resistivity ρ_c. These crystallites are separated by thin dielectric partitions which provide an effective resistivity ρ_b to electron current. The total series resistivity ρ of the crystallite and barrier is

$$\rho = \rho_b + \rho_c. \qquad (17)$$

The film resistivity is much larger than that of the crystallites, $\rho_b \gg \rho_c$, therefore ρ_c can be neglected in comparison with ρ_b in the expression for the macroscopic conductivity of the photosensitive film. The current voltage relationship for the barrier is

$$j = M\rho_b e^{-\frac{q\phi}{kT}}\left(e^{\frac{q\Delta V_b}{kT}} - 1\right), \qquad (18)$$

where j is the current density, q the charge of a carrier, ρ_b the mean density of majority carriers in the bulk, i.e. the crystallites, ϕ is the effective potential height of the barriers relative to the valence band edge, k Boltzman's constant, T the absolute temperature, ΔV_b the voltage drop across the barrier, and M a parameter dependent on the specific nature of the barrier but independent of ϕ. Because of the microscopic dimensions of the crystallites the voltage per crystallite is so small that $\Delta V_b \ll q/kT$. The barrier current-voltage relationship can then be written as

$$j = M\rho_b e^{-\frac{q\phi}{kT}} q\frac{\Delta V_b}{kT}. \qquad (19)$$

The conductivity σ of a film of length ℓ is given by

$$\sigma = j\ell/V_b, \qquad (20)$$

where V_b is the voltage drop across the film and is related to the barrier voltage ΔV_b by

$$V_b = \ell n \Delta V_b, \qquad (21)$$

where n is the number of barriers or crystals per cm. From Eqs. (19), (20), and (21)

$$\sigma = M p_b e^{\frac{-q\phi}{kT}} q/nkT = q p_b \mu_p. \qquad (22)$$

From Eq. (22) we find that

$$\mu_p = M e^{\frac{-q\phi}{kT}}/nkT, \qquad (23)$$

where μ_p is the effective mobility of the p-type film. Breaking Eq. (23) down

$$\mu_p = \mu e^{\frac{-q\phi}{kT}}, \qquad (24)$$

$$\mu = M/nkT \qquad (25)$$

where μ is the mobility of the holes independent of the potential hill at the barrier and $e^{-q\phi/kT}$ accounts for the reduction in mobility caused by the potential hill of the barrier. From Eq. (22) the conductance and the resistance are

$$G = \frac{1}{R} = \frac{wd}{l}\sigma = \frac{wd}{lkT} q M p_b e^{\frac{-q\phi}{kT}}, \qquad (26)$$

where w and d are the film width and thickness respectively.

3. Photoconductivity: According to the majority carrier model, photoconductivity in the lead-salt type of thin films results when photons of sufficient energy enter the

crystallites and create excess hole-electron pairs by exciting main band transitions. The excess electrons are trapped, thus permitting the relatively long hole lifetimes required to explain photoconductivity. While the trapped electrons are immobile and cannot contribute directly to the photocurrent, they might affect the barrier potential ϕ. If the light source has sufficiently small intensity so that the fractional change in the density of holes is small and if the possibility of barrier modulation is admitted, the conductance change resulting from the photon induced holes Δp_b is given by

$$\Delta\sigma = q\mu_p \Delta p_b + q p_b \Delta\mu_p. \qquad (27)$$

The total change in density of majority carriers in the crystallites is assumed to contribute to the change in conductivity. This assumption requires a minority carrier diffusion length which is long compared to the crystallite dimensions. Long diffusion length for the minority carriers means that the photon created hole-electron pairs do not recombine instantaneously. A parameter B_p is selected to characterize the relative effect of barrier modulation on the conductivity in comparison with the effect of Δp_b by the following equation

$$B_p = \left(\frac{\Delta\mu_p}{\mu_p}\right)\Big/\left(\frac{\Delta p_b}{p_b}\right). \qquad (28)$$

Equation (27) may then be written as

$$\Delta\sigma = q\mu_p(1 + B_p)\Delta p_b. \qquad (29)$$

The rate equation for the photon injected holes is

$$\frac{d\Delta p_b}{dt} + \frac{\Delta p_b}{\tau_p'} = g. \qquad (30)$$

τ_p' is the lifetime of the photon produced holes. The rate of creation of hole-electron pairs per unit volume by absorption of the incident photons, is given by

$$g = \eta J/h\nu d, \qquad (31)$$

where J is the incident signal light flux in watts per cm^2, $h\nu$ is the energy per photon, and η is the probability that an incident photon will excite a hole-electron pair. According to Rittner[2] the carriers can be assumed to be produced uniformly throughout the crystallites. τ_p' can then be written in terms of the bulk trapping time τ_b and the effective surface recombination time τ_s as

$$\frac{1}{\tau_p'} = \frac{1}{\tau_b} + \frac{1}{\tau_s}. \qquad (32)$$

In the case of a thin sheet-like single crystal semiconductor, τ_s is expressed in terms of a recombination velocity S and the crystal thickness d as

$$\tau_s = \frac{d}{2S}. \qquad (33)$$

In the case where the film is a composite of crystallites, τ_s is proportional to d/2S where d is a representative crystallite dimension.

If the light is switched on at t=0, the solution of the rate equation (30) is

$$\Delta p_b = g\tau_p'\left(1 - e^{-\frac{t}{\tau_p'}}\right), \qquad (34)$$

If Eq. (34) is placed into Eq. (29), we obtain the change in conductance

$$\Delta\sigma = q\mu_p(1+B_p)g\tau_p'\left(1 - e^{-\frac{t}{\tau_p'}}\right). \qquad (35)$$

The corresponding response to incident light pulsed or chopped at an angular frequency ω is

$$\Delta\sigma = \frac{q\mu_p(1+B_p)g\tau_p'}{(1+\omega^2\tau_p'^2)^{\frac{1}{2}}}. \qquad (36)$$

In a film of length ℓ, width w, and thickness d, the change in conductance ΔG is

$$\Delta G = \frac{wd}{\ell}\Delta\sigma. \qquad (37)$$

The output voltage ΔV_o of the balanced bridge in response to a conductance change ΔG in the film is given in Eq. (1). Using Eqs. (1), (35) and (37), we find that the transient voltage response is

$$\Delta V_o = -q(1+B_f)\mu_f g \tau_f' \frac{wd}{l} \frac{I_s R^2 (R_1+R_2)}{(R_1+R_2+R)} (1+e^{-\frac{t}{\tau_f}}). \quad (38)$$

The relation between beat-frequency bridge response V_w and a change ΔR in film resistance is given in Eq. (3). Since $\Delta R = R^2 \Delta G$, Eqs. (3), (36), and (37) yield

$$V_w = (1+B_f)\mu_f g q \tau_f' \frac{wd}{l} \frac{RV_b}{\sqrt{2} L_w} \frac{1}{(1+\omega^2 \tau_f'^2)^{\frac{1}{2}}}. \quad (39)$$

We restate for emphasis that the response, either Eq. (38) for transients or Eq. (39) for steady state ac, which this theory predicts should be observed experimentally is proportional to the rate of generation and lifetime of the holes (majority carrier). The direct contribution of electrons to photoconductivity is ignored. In fact, we assumed that although incident photons create hole-electron pairs the electrons are immediately trapped and only the photo-holes live long enough to affect the conductivity.

4. Field Effect: The majority carrier model is now extended to describe the field effect. In studying the field effect phenomena, the field effect plate is capacitively coupled to the film. A voltage difference between the field effect plate and the film induces excess positive charge either into or out of the film depending on the polarity of the voltage. Let Δp be the total number of excess positive charges induced per unit film area exposed to the field effect plate. Of these charges Δp_b are assumed to be mobile in the space charge region of the bulk and Δp_t are trapped.

We use the term "trapped" to designate those excess charges which are immobilized at sites either on the surface or in the space charge region. According to the law of conservation of charge

$$\Delta p = \Delta p_b + \Delta p_t , \quad (40)$$

Δ signifies an excess over the equilibrium value for zero field effect voltage. Δp_b causes an incremental change $\Delta \sigma_s$ in conductance per unit area. From arguments similar to those used to obtain the change in conductivity due to photoconductivity,

$$\Delta \sigma_s = \Delta p_b q (1+B_f) \mu_f , \quad (41)$$

where B_f results from field induced barrier modulation and μ_f is the effective mobility of the excess holes in the space charge region. This definition of μ_f is to be contrasted with one often used in surface state physics which defines the effective mobility on the basis of all the induced charges. In the latter case $\mu_{fe} = \Delta \sigma_s / q \Delta p$, where Δp is the surface density of excess charges including those which are trapped as well as those which are mobile. The excess charges Δp_t are bound and do not contribute directly to the measured conductance change of the film; however, these charges terminate electric field lines from the field effect plate.

The induced charges enter the film through the terminals. If charge enters the traps only from the space change conduction region, the time rate of increase in trap occupancy is given by

$$\frac{d}{dt}\Delta p_t = \frac{\Delta p_b}{\tau_{bt}} - \frac{\Delta p_t}{\tau_{tb}} , \qquad (42)$$

where $1/\tau_{bt}$ is the probability of an excess carrier transferring from the space charge region to a trap in a second, and $1/\tau_{tb}$ is the probability per second that an excess surface charge will transfer from a trap to the space charge region.

A time derivative of Eq. (40) yields a continuity equation;

$$\frac{d}{dt}\Delta p = \frac{d}{dt}\Delta p_b + \frac{d}{dt}\Delta p_t . \qquad (43)$$

This can be written in terms of the effective time constants τ_{tb} and τ_{bt} by using Eq. (42). The time rate of change of excess charge carriers in the space charge region is given by

$$\frac{d}{dt}\Delta p_b = \frac{d}{dt}\Delta p - \frac{\Delta p_b}{\tau_{bt}} + \frac{\Delta p_t}{\tau_{tb}} . \qquad (44)$$

If Eq. (40) is placed in Eq. (44), Δp_t can be eliminated and

$$\frac{d}{dt}\Delta p_b + \left(\frac{1}{\tau_{bt}} + \frac{1}{\tau_{tb}}\right)\Delta p_b = \frac{d}{dt}\Delta p + \frac{\Delta p}{\tau_{tb}} . \qquad (45)$$

New parameters τ_f' and α' are now defined as

$$\frac{1}{\tau_f'} = \frac{1}{\tau_{bt}} + \frac{1}{\tau_{tb}} , \qquad (46)$$

and

$$\alpha' = \tau_f'/\tau_{bt} . \qquad (47)$$

It follows that

$$\tau_{tb} = \frac{\tau_f'}{1-\alpha'} . \qquad (48)$$

If the new parameters are placed in Eq. (45), the resulting simplified equation is

$$\frac{d}{dt}\Delta p_b + \frac{\Delta p_b}{\tau_f'} = \frac{d}{dt}\Delta p + \frac{1-\alpha'}{\tau_f'}\Delta p . \qquad (49)$$

Consider the solution to the rate equation (49) in response to a step-function field effect voltage which is zero up to time t = 0 and some value V_f thereafter. The total induced charge is

$$\Delta p = 0 \quad \text{at} \quad t < 0 , \qquad (50)$$

and

$$\Delta p = -kV_f \quad \text{at} \quad t \geq 0 , \qquad (51)$$

where k is the charge induced per unit area per field effect volt, i.e. the field effect plate to film capacity per unit area. Since

there are no excess charges in the film bulk prior to the initiation of the field effect voltage,

$$\Delta p_b = 0 \quad \text{at} \quad t < 0. \tag{52}$$

At the initiation of the field effect voltage, all of the induced charges Δp are assumed to appear instaneously as excess carriers, i.e.

$$\Delta p_b = -k V_f \quad \text{at} \quad t = 0. \tag{53}$$

With the boundary conditions of Eqs. (52) and (53) imposed, the solution to Eq. (49) is

$$\Delta p_b = -k V_f \left[(1-\alpha') + \alpha' e^{-\frac{t}{\tau_f'}}\right]. \tag{54}$$

If this is substituted into Eq. (41), the change in surface conductivity with time is

$$\Delta \sigma_s = -k V_f (1+B_f) \mu_f q \left[(1-\alpha') + \alpha' e^{-\frac{t}{\tau_f'}}\right]. \tag{55}$$

The change ΔG in conductance of a film exposed to a field effect plate of length ℓ and width w is,

$$\Delta G = \frac{w}{\ell} \Delta \sigma_s . \tag{56}$$

For this same film with a field effect plate to film capacity C_f

$$k = C_f / w\ell. \tag{57}$$

From Eqs. (55), (56) and (57), the total conductance change in the film is then:

$$\Delta G_{ft} = -V_f \frac{(1+B_f)\mu_f q C_f}{\ell^2} \left[(1-\alpha') + \alpha' e^{-\frac{t}{\tau_f'}}\right] \tag{58}$$

and if measured in the balanced bridge described in II.B.1., the response voltage is

$$\Delta V_o = V_f (1+B_f) \mu_f C_f q \frac{I_3 R^2 (R_1+R_2)}{\ell^2 (R_1+R_2+R)} \left[(1+\alpha) + \alpha e^{-\frac{t}{\tau_f}}\right]. \tag{59}$$

Equation (59) predicts the transient response of the type shown in Figs. 13 and 28. At the start of the negative field effect voltage, excess holes (majority carriers) are induced into the space charge region of the crystallite. These excess holes flow into film through the film terminals in order to achieve overall charge neutrality of the film and field effect plate. The electric field from the field effect plate attracts the excess holes into the space charge region where their presence both increases the conductance and upsets the equilibrium of the traps. These surface and/or space traps tend toward equilibrium by a net transfer of charge. In keeping with Gauss's theorem, 4π of the electric lines of force of the transverse electric field terminate on each trap which has effectively immobilized a hole, (see Fig. 27). The nature of these traps

will be discussed further in Chapter IV. The experimentally observed exponential decay results from this net transfer of induced holes to the traps. At quasi-equilibrium a fraction α of the induced holes is trapped. The term quasi-equilibrium is used to acknowledge the presence of slow states which require much longer times to achieve equilibrium. When the field effect voltage is suddenly removed, the excess surface density of holes in the space charge region is decreased causing a corresponding decrease in conductance. Since the traps cannot transfer charge instantaneously, they momentarily have an excess of positive charge. The net transfer of this charge to the space charge region causes the observed exponential rise of film conductance. The description of response to a positive square wave field effect voltage is similar except that at the start of the voltage pulse, holes are induced out of the space charge region. Note that in the analysis we assume the RC charging time to be vanishingly small, in agreement with the experimental conditions. We also neglect the time involved for charge to enter the space charge region; this time is the dielectric relaxation time which is of the order of 10^{-12} seconds and therefore completely negligible.

Consider now the solution to the rate equation (49) when the field effect voltage is sinusoidal. The density of excess charge Δp induced by the field effect voltage V_f is then given by the real part of

$$\Delta p = -k \hat{V}_f e^{i\omega t}. \tag{60}$$

The time derivative is

$$\Delta \dot{p} = +i\omega \Delta p, \tag{61}$$

and the rate eq. (49) becomes

$$\Delta \dot{p}_b + \frac{\Delta p_b}{\tau_f} = -\left(i\omega + \frac{1-\alpha'}{\tau_f'}\right) k \hat{V}_f e^{i\omega t}. \tag{62}$$

If we assume a solution to Eq. (62) of the form

$$\Delta p_b = -A e^{i(\omega t + \theta)}, \tag{63}$$

the time derivative is

$$\Delta \dot{p}_b = +i\omega \Delta p_b \tag{64}$$

and Eq. (62) becomes

$$\left(i\omega + \frac{1}{\tau_f}\right) A e^{i(\omega t+\theta)} = \left(i\omega + \frac{1-\alpha'}{\tau_f'}\right) k \hat{V}_f e^{i\omega t}, \tag{65}$$

from which

$$A e^{i\theta} = k \hat{V}_f \left(\frac{i\omega\tau_f' + 1 - \alpha'}{i\omega\tau_f' + 1}\right). \tag{66}$$

Then A is given by

$$A = k \hat{V}_f \frac{\left[(1-\alpha+\omega^2\tau_f^2)^2 + \alpha^2\omega^2\tau_f'^2\right]^{\frac{1}{2}}}{\omega^2\tau_f'^2 + 1}, \tag{67}$$

and θ is

$$\theta = \tan^{-1}\left(\frac{\alpha\omega\tau_f'}{\omega^2\tau_f'^2+1-\alpha'}\right) . \qquad (68)$$

By placing the values of A and θ from Eqs. (67) and (68) into Eq. (63) the density and phase of excess holes in the bulk in response to the field effect voltage is

$$\Delta p_b = -k\hat{V}_f \frac{\left[(1-\alpha+\omega^2\tau_f'^2)^2+\alpha'^2\omega^2\tau_f'^2\right]^{\frac{1}{2}}}{\omega^2\tau_f'^2+1} e^{i(\omega t+\theta)} \qquad (69)$$

By substituting Eq. (69) into Eq. (41) and the results into Eq. (56) we find the change in film conductance to be

$$\Delta G_{fs} = \frac{-(1+B_f)\mu_f q C_f}{l^2}\hat{V}_f \frac{\left[(1-\alpha'+\omega^2\tau_f'^2)^2+\alpha'^2\omega^2\tau_f'^2\right]^{\frac{1}{2}}}{\omega^2\tau_f'^2+1} e^{i(\omega t+\theta)} \qquad (70)$$

The theoretical equation for F_f is then

$$F_f = \frac{(1+B_f)\mu_f q C_f R}{l^2} \frac{\left[(1-\alpha'+\omega^2\tau_f'^2)^2+\alpha'^2\omega^2\tau_f'^2\right]^{\frac{1}{2}}}{\omega^2\tau_f'^2+1} e^{i\theta} . \qquad (71)$$

In this study, τ_f' and α' were evaluated from the relative amplitude of Eq. (71) as a function of frequency. Equations (71) and (3) predict

$$V_w = \frac{V_f V_b F_f}{\sqrt{2}\, L_w} \qquad (72)$$

$$= V_f V_b \frac{(1+B_f)\mu_f q C_f R}{\sqrt{2}\, L_w l^2} \frac{\left[(1-\alpha'+\omega^2\tau_f'^2)^2+\alpha'^2\omega^2\tau_f'^2\right]^{\frac{1}{2}}}{\omega^2\tau_f'^2+1} .$$

Equation (72) predicts the measured steady state ac field effect response, e.g. Fig. 24. The reason for the maximum response at high frequency is that the traps do not have time to capture the excess charges induced by the field effect during a cycle. All induced charges are then mobile and contribute directly to the induced conductance change. At low frequency, the traps have time to capture α' of the induced charge. The response is then reduced by a fraction α' from that at high frequency. The transition between maximum and minimum indicates the fraction of induced charges which are trapped per cycle as a function of frequency.

C. Comparison of Empirical And Theoretical Equations

1. Photoresponse: Equations (14) and (38), the empirical and theoretical equations for describing the transient photoresponse as measured with the balanced bridge, are identical if $\tau_p = \tau_p$ and

$$(1+B_p)\mu_p = -G_{pt}\frac{l(R_1+R_2+R)}{q\tau_p w d I_s R^2(R_1+R_2)} . \qquad (73)$$

Equations (15) and (39), the empirical and theoretical equations for describing the steady state ac photoresponse as measured with the beat frequency bridge, are identical if $\tau_p = \tau_p$ and

$$(1+B_p)\mu_p = \frac{G_{ps}}{V_b}\frac{\sqrt{2}\, L_w l}{q\tau_p w d R} . \qquad (74)$$

Because of the agreement between theory and experiment indicated in the previous comparisons, τ_p will be used in place of τ_p in further discussions.

2. Field Effect: The empirical equation (6) and the theoretical equation (59) are identical if $\alpha = \alpha'$, $\tau_f = \tau_f'$, and the mobility product is

$$(1+B_f)\mu_f = G_{ft}\frac{\ell^2(R_1+R_2+R)}{C_f q I_s R^2(R_1+R_2)} \quad . \quad (75)$$

Also Eqs. (8) and (72), the empirical and theoretical equations for describing steady state ac field effect are identical if $\alpha = \alpha'$, $\tau_f = \tau_f'$ and

$$(1+B_f)\mu_f = \frac{\sqrt{2}\,L_w \ell^2 G_{fs}}{q C_f R V_b} \quad . \quad (76)$$

All of the parameters on the right side of Eqs. (75) and (76) can be determined by electrical or physical measurements. From the agreement between the theoretical and empirical equations, we conclude that the extended majority carrier model describes field effect in the PbS films. α and τ_f will replace α' and τ_f in further discussions.

IV. INTERPRETATION OF EXPERIMENTAL DATA

A. General

In this section, the experimental data is applied to a series of basic problems of the physics of photoconductivity in PbS films for the purpose of specifying in more detail the mechanism of photoconductivity.

B. Majority Versus Minority Carrier Lifetime

As stated in the introduction an important question in photoconductivity is whether the recombination process (lifetime) is minority or majority carrier limited in infrared sensitive lead salt type films. The majority carrier model[1] assumes the process to be majority carrier limited, i.e. the experimental photoresponse time constant is the majority carrier lifetime. Field effect experiments reported herein are the most direct evidence yet in support of this assumption. The reasoning is very simple in the case of surfaces, such as those envisaged on the PbS films, with nearly flat or accumulation type space charge regions; in the field effect measurements one induces only majority carriers and observes their lifetime. Since the experimental field effect and photoresponse time constants are identical, i.e. $\tau_p = \tau_f$, one concludes that τ_p is also a majority carrier lifetime. If the photoconductive process were minority carrier limited, there would have been little correlation between τ_p and τ_f.

In summary, the identity of the experimental field and photoresponse time constants, when considered together with a large number of other experiments[11,17,18,19], substantually confirm the majority carrier model for photoconductivity in PbS films

C. Rate Limiting Process

Our next objective is to determine the rate limiting process for net transfer of charge into and out of the photoconductive traps. Equation (46) provides the field effect time constant τ_f in terms of the time constants τ_{bt} and τ_{tb} for hole transfer into and out of the traps probed by the field effect. Equations (47) and (48) relate τ_{bt} and τ_{tb} to the measured values of τ_f and α. In a sensitized film α is of the order of 0.9 which means that $\tau_f \cong \tau_{bt}$ and that $\tau_{tb} \gg \tau_{bt}$.

The conclusion is then that the rate limiting process for majority carrier trapping in a sensitized film is the rate of transfer of charge from the space charge region to the traps. From the identity of the field effect and photoresponse time constants, we further conclude that the rate limiting process for photoconductivity is the same as for field effect.

D. Estimate of Trap Densities And Capture Cross-sections

Field effect data will now be used to estimate the effective density and cross-sections of the hole traps. We will consider only those traps and holes which are influenced by the field effect measurements. The total rate at which holes in equilibrium enter the traps probed by field effect is

$$R_{b\to t} = \bar{p}_b / \tau_{bt} , \qquad (77)$$

where $\bar{p}_b$ is the mean density of conducting holes in the space charge region and $1/\tau_{bt}$ is the transition rate per hole from space charge region to traps. The total rate of hole transfer from traps to the valence band in the space charge region is

$$R_{t\to b} = \bar{p}_t / \tau_{tb} , \qquad (78)$$

where $\bar{p}_t$ is the mean volume density of occupied hole traps in the region probed by field effect and $1/\tau_{tb}$ is the transition rate per hole from trap to valence band. Although $\bar{p}_t$ is stated as a mean volume density, it can readily be converted to a surface density as shown later. At thermal equilibrium

$$R_{b\to t} = R_{t\to b} \qquad (79)$$

therefore,

$$\bar{p}_b / \tau_{bt} = \bar{p}_t / \tau_{tb} . \qquad (80)$$

In our case

$$\bar{p}_b = N_v e^{-\frac{(E_v - E_f)}{kT}} , \qquad (81)$$

and

$$\bar{p}_t = \frac{N_t}{1 + e^{-\frac{(E_t - E_f)}{kT}}} , \qquad (82)$$

where N_v is the effective density of states for holes in the valence band; N_t is the mean density of traps probed by field effect; and E_v, E_f, and E_t are the energy levels for the valence band, Fermi level, and traps respectively. Because of the control of the Fermi level by the traps we assume $E_f \cong E_t$. Equations (81) and (82) then become

$$\bar{p}_b \cong N_v e^{-\frac{E_{tv}}{kT}} \qquad (83)$$

and

$$\bar{p}_t \cong N_t/2 , \tag{84}$$

where E_{tv}, as shown in Figs. 3 and 4, is $E_t - E_v$.

From Eqs. (80), (83), and (84) we obtain

$$\frac{\tau_{bt}}{\tau_{tb}} = \frac{\bar{p}_b}{\bar{p}_t} = \frac{2N_v}{N_t} e^{-\frac{E_{tv}}{kT}} \tag{85}$$

From Eqs. (47) and (48) we know that

$$\frac{\tau_{bt}}{\tau_{tb}} = \frac{1-\alpha}{\alpha} . \tag{86}$$

The mean density of the traps sampled by field effect is then

$$N_t = \frac{2\alpha N_v}{1-\alpha} e^{-\frac{E_{tv}}{kT}} . \tag{87}$$

We note that this expression is independent of τ_f. However, the cross-sections for the traps can only be obtained by measuring both τ_f and α.

The capture cross-section of the trap is

$$\sigma_{bt} = \frac{1}{\tau_{bt} v (N_t - \bar{p}_t)} , \tag{88}$$

where v is the thermal velocity of the holes. From Eqs. (47), (84), and (88) we find

$$\sigma_{bt} \cong \frac{1-\alpha}{\tau_f v N_v} e^{\frac{E_{tv}}{kT}} . \tag{89}$$

We shall now estimate the trap densities and trapping cross-section of a typical sensitized film. First the effective number of states for holes in the valence band is

$$N_v = 2(2\pi m_p kT/h^2)^{3/2} , \tag{90}$$

where m_p, k, T, and h are the effective mass of the hole, Boltzmann's constant, absolute temperature, and Planck's constant respectively. At room temperature (20°C) if m_p is assumed to be unity we find

$$N_v = 2.4 \times 10^{19}/cm^3 . \tag{91}$$

Placing this density for N_v and 0.11 electron volts for ΔE_{tv} as obtained from Fig. 3 into Eq. (87) we obtain

$$N_t \cong \frac{6\alpha}{1-\alpha} \times 10^{17}/cm^3 . \tag{92}$$

Since the thermal velocity v is approximately 10^7 cm/sec, we have

$$\sigma_{bt} \cong \frac{3.4\,(1-\alpha)}{\tau_f} \times 10^{-25}\ cm^2. \qquad (93)$$

Typical measured values of α and τ_f for uncoated sensitized films are 0.9 and 300 microseconds respectively. Typical average volume densities and cross-sections for traps indicated by Eqs. (92) and (93) are

$$N_t \cong 5 \times 10^{18}/cm^3 \qquad (94)$$

$$\sigma_{bt} \cong 1 \times 10^{-22}/cm^2. \qquad (95)$$

If the traps are located entirely in the bulk, i.e. negligible surface trapping, the bulk density of traps as indicated by Eq. (94) is quite large. Rose[3] states that trap densities of this order of magnitude are conceivable; however, above these densities impurity bands form.

If the traps are located on the film surface, i.e. at the oxide interface of the crystallites, if the characteristic dimension of the crystallite d_c is much larger than L_D, and if $L_D \cong 0.1$ microns; the surface density of states would be

$$N_{ts} = L_D N_t \cong 5 \times 10^{13}/cm^2. \qquad (96)$$

If $d_c < L_D$, then the surface density of states on the crystallites would be

$$N_{ts} \cong d_c N_t \cong \frac{d_c}{L_D} 5 \times 10^{13}/cm^2. \qquad (97)$$

Densities of surface traps of the order indicated in Eq. (96) are reasonable. One reason is that the traps probably arise from oxidation at the crystallite interface. If all of the oxide in contact with the interface were effective as traps then densities of the order of $10^{14}/cm^2$ would be expected. Surface densities of the order indicated in Eq. (97) are even more reasonable.

Assuming the traps to be located on the surface and $d_c > L_D$, the surface trapping velocity is

$$S_{ss} = \nu \sigma_{bt} \frac{N_t - \bar{P}_t}{L_D} \sim 3 \times 10^{-2}\ cm/sec \qquad (98)$$

If $d_c < L_D$ then the trapping velocity of the crystallite surface is

$$S_{ss} = \nu \sigma_{bt} \frac{N_t - \bar{P}_t}{d_c} \sim \frac{L_D}{d_c} 3 \times 10^{-2}\ cm/sec \qquad (99)$$

The cross-section estimated in Eq. (95) is quite small which suggests the traps could be a positively charged site. The Coulomb force would repel the hole causing the long hole lifetimes measured in field effect and photoconductivity.

In summary, the measurement of α and τ_f by field effect, allows for estimates of trap densities and trapping cross-sections. In contrast, photoresponse measurements provide only τ_p from which only the product of density and cross-section can be calculated. Thus field effect measurements are an important tool in the study of the photoconductive process of the thin films.

E. Location of Photoconductive Traps

We assume that the film is a homogeneous polycrystalline structure. An average crystallite has a characteristic dimension d_c which is related to the crystallite volume

$$V_c = A_c d_c , \tag{100}$$

where A_c is the total area of the crystallite. Since the space charge region extends approximately a distance L_D beneath the crystallite surface, the volume occupied by this region is

$$V_{sc} = A_c L_D . \tag{101}$$

The volume in the crystallite exterior to the space charge region is then

$$V_{be} = A_c (d_c - L_D) \tag{102}$$

provided $d_c > L_D$, otherwise $V_{be} = 0$. The following definitions are required for further discussion:

N_{be} = bulk states in V_{be} / cm^3 (unoccupied)
N_{sc} = bulk states in V_{sc} / cm^3 (unoccupied)
N_{ss} = states on surface / cm^2 (unoccupied)

σ_{be} = effective cross-section for trapping holes in V_{be}
σ_{sc} = effective cross-section for trapping holes in V_{sc}
σ_{ss} = effective cross-section for trapping holes in surface state.

If we assume crystallites of uniform properties we can define the following lifetime parameters:

$$1/\tau_{be} = \nu \sigma_{be} N_{be} , \tag{103a}$$

$$1/\tau_{sc} = \nu \sigma_{sc} N_{sc} , \tag{103b}$$

and

$$S_{ss} = \nu \sigma_{ss} N_{ss} , \tag{103c}$$

where $1/\tau_{be}$ and $1/\tau_{sc}$ are the probability density for capture of charge in a trap in V_{be} and V_{sc} respectively, S_{ss} is the surface trapping velocity and v is the thermal velocity of the majority carriers.

If we postulate that the majority carriers are uniformly distributed throughout a crystallite, the transition rates for hole capture in an average crystallite are

$$\frac{1}{\tau_{be}'} = \nu \sigma_{be} N_{be} V_{be} / V_c = \frac{1}{\tau_{be}} \frac{d_c - L_D}{d_c} , \tag{104a}$$

$$\frac{1}{\tau_{sc}'} = \frac{\nu \sigma_{sc} N_{sc} V_{sc}}{V_c} = \frac{1}{\tau_{sc}} \frac{L_D}{d_c} , \qquad (104b)$$

$$\frac{1}{\tau_{ss}'} = \frac{\nu \sigma_{ss} N_{ss} A_c}{V_c} = \frac{S_{ss}}{d_c} . \qquad (104c)$$

The total probability density for hole capture in the crystallite is

$$\frac{1}{\tau_{bt}}\Big|_c = \frac{1}{\tau_{be}'} + \frac{1}{\tau_{sc}'} + \frac{1}{\tau_{ss}'} . \qquad (104d)$$

If hole trapping is the rate limiting process in the net transfer of charge in a sensitized film, then the photoresponse time of the crystallite for $d_c > L_D$ is

$$\frac{1}{\tau_p}\Big|_c = \frac{1}{\tau_{bt}}\Big|_c + \frac{1}{\tau_{tb}}\Big|_c \cong \frac{1}{\tau_{bt}}\Big|_c . \qquad (105)$$

We neglect the effect of τ_{tb} in the following analysis for reasons discussed in Section C above. From Eqs. (104a, b, c, d) and (105) the photoresponse time of the crystallite in terms of its lifetime parameters and characteristic dimensions is

$$\frac{1}{\tau_p}\Big|_c = \frac{1}{\tau_{be}}\left(1 - \frac{L_D}{d_c}\right) + \frac{1}{\tau_{sc}}\frac{L_D}{d_c} + \frac{S_{ss}}{d_c} . \qquad (106)$$

We next determine the photoresponse time constant for the film as a composite of crystallites. Let N be the volume density of crystallites and assume the majority carriers

to be equally distributed throughout all crystallites. The probability densities for trapping a majority carrier in the bulk states exterior to the crystallite space charge region, the space charge region, and in the surface states respectively are

$$\frac{1}{\tau_{bc}''} = \frac{\nu \sigma_{be} N_{be} V_{be} N}{V_c N} = \frac{1}{\tau_{be}'} , \qquad (107a)$$

$$\frac{1}{\tau_{sc}''} = \frac{\nu \sigma_{sc} N_{sc} V_{sc} N}{V_c N} = \frac{1}{\tau_{sc}'} , \qquad (107b)$$

$$\frac{1}{\tau_{ss}''} = \frac{\nu \sigma_{ss} N_{ss} A_c N}{V_c N} = \frac{1}{\tau_{ss}'} . \qquad (107c)$$

The photoconductive time constant $\tau_p|_F$ for the film is then obtained from

$$\frac{1}{\tau_p}\Big|_F = \frac{1}{\tau_{be}''} + \frac{1}{\tau_{sc}''} + \frac{1}{\tau_{ss}''} . \qquad (108)$$

We now see that the film and crystallite time constants are equal:

$$\frac{1}{\tau_p}\Big|_F = \frac{1}{\tau_p}\Big|_c = \frac{1}{\tau_{be}}\left(1 - \frac{L_D}{d_c}\right) + \frac{1}{\tau_{sc}}\frac{L_D}{d_c} + \frac{S_{ss}}{d_c} . \qquad (109)$$

To obtain the field effect time constant, we postulate that the induced majority carriers are restricted to a region L_D within the surface of the film facing the field effect plate. If $L_D < d_c$, the probability densities for induced charge trapping in the surface states and in the space charge region are, respectively,

$$\frac{1}{\tau_{ss}'''} = \frac{v\sigma_{ss} N_{ss} A_F}{A_F L_D} = \frac{S_{ss}}{L_D} \qquad (110a)$$

and

$$\frac{1}{\tau_{sc}'''} = \frac{v\sigma_{sc} N_{sc} A_F L_D}{A_F L_D} = \frac{1}{\tau_{sc}} , \qquad (110b)$$

where A_F is the area of the film exposed to the field effect plate. The field effect time constant for the film in terms of lifetime parameters and characteristic dimensions is then

$$\left.\frac{1}{\tau_f}\right|_F = \frac{S_{ss}}{L_D} + \frac{1}{\tau_{sc}} . \qquad (111)$$

We note that the $1/\tau_f \,|_F$ does not depend on τ_{be}, that is trapping in bulk states exterior to the space charge regions.

Consider now the case where $L_D > d_c$. By reasoning similar to that above we can show that

$$\left.\frac{1}{\tau_p}\right|_F = \frac{1}{\tau_{sc}} + \frac{S_{ss}}{d_c} \qquad (112)$$

and

$$\left.\frac{1}{\tau_f}\right|_F = \frac{1}{\tau_{sc}} + \frac{S_{ss}}{d_c} . \qquad (113)$$

The principal Eqs. (109), (111), (112) and (113) derived in this section are collected in the following table in which we no longer carry the subscript F:

Case		Field Effect	Photoresponse
$d_c \geq L_D$	$\tau_{sc} \neq \tau_{be}$	$\frac{1}{\tau_f} = \frac{1}{\tau_{sc}} + \frac{S_{ss}}{L_D}$	$\frac{1}{\tau_p} = \frac{1}{\tau_{sc}}\frac{L_D}{d_c} + \frac{1}{\tau_{be}}\left(1-\frac{L_D}{d_c}\right) + \frac{S_{ss}}{d_c}$
$d_c \geq L_D$	$\tau_{sc} = \tau_{be}$	$\frac{1}{\tau_f} = \frac{1}{\tau_{sc}} + \frac{S_{ss}}{L_D}$	$\frac{1}{\tau_p} = \frac{1}{\tau_{sc}} + \frac{S_{ss}}{d_c}$
$d_c \leq L_D$	$N_{be} = 0$	$\frac{1}{\tau_f} = \frac{1}{\tau_{sc}} + \frac{S_{ss}}{d_c}$	$\frac{1}{\tau_p} = \frac{1}{\tau_{sc}} + \frac{S_{ss}}{d_c}$

These results can be used to derive information from measurements of τ_f and τ_p. Consider for example that we know τ_f, τ_p, L_D and d_c, where in general $\tau_f \neq \tau_p$. Assume further that $d_c > L_D$. Then from line one in the table we have two simultaneous equations involving three unknowns, τ_{sc}, τ_{be} and S_{ss}. Thus we can find two of the unknowns in terms of the third. If one can assume that $\tau_{sc} = \tau_{be}$, as would be true if the space charge potential does not differ radically from the bulk potential, then from line two we can find τ_{sc} and S_{ss}. That is, we can separate the effects of bulk and surface trapping. When $d_c \leq L_D$ line three shows that we expect that $\tau_f = \tau_p$ and we cannot separate τ_{sc} from S_{ss} by these measurements.

The above discussion illustrates the general usage of the table; we now apply our experimental result that $\tau_f = \tau_p$ to derive further information. From line three of the table we see that one expects $\tau_f = \tau_p$ if $d_c \leq L_D$. This may well be the case for these films although we do not have data available on crystallite size. For this case we cannot achieve a further separation between τ_{sc} and S_{ss} from simply field effect and photoconductive measurements. However, our estimates of the bulk and surface densities in Section C above favor surface over bulk traps. The reason being that for bulk traps one needs a density $N_t = 5 \times 10^{18}/cm^3$, while for surface traps the

density required is $N_{ts} \cong 5 \times 10^{13}$ cm. While both densities are possible, past experience in other photoconductors[3] would tend to favor the surface density. However, further study is needed to clarify this point and it may well be that both bulk and surface traps are important.

If the crystallites are much larger than a Debye length ($d_c \gg L_D$), then the data of $\tau_f = \tau_p$ indicates that bulk traps are dominant. This is shown in line two of the table where we also assume $\tau_{sc} \cong \tau_{be}$.

F. Evidence Concerning Barrier Modulation

The field effect measurements give supporting evidence that the majority carrier model can be based entirely on changes in the number of majority carriers in the crystallites, i.e. barrier modulation of the effective mobility by small densities of excess carriers is negligible. This result was previously established by Woods[19] who compared the change in resistivity with the change in Hall coefficient under illumination. Confirmation of Wood's results is based on the agreement between the measured field effect mobility and the Hall mobility in these films (See Section II-D.3 where $B_f = 0$).

Our experiment is not entirely equivalent to Woods' since the field effect induces only majority carriers, while Woods used radiation, which induces both majority and minority carriers. Stated more precisely, the field effect shows that there is no barrier modulation resulting from changes in the density of majority carriers. Woods' experiment showed that there is no barrier modulation resulting when both minority and majority carriers are generated by light. Taken together the two experiments strongly support the model of photoconductivity based purely on a change in the density of majority carriers; no barrier modulation or mobility modulation occurs.

The homogeneous model also suggests that the field effect mobility product $(1 + B_f)\mu_f$ should be approximately equal to the Hall mobility. The point being that the space charge region adjacent to the outer surface of the film is representative of the crystallites throughout the film. Thus one expects the same mobility from field effect as from Hall effect as was found to be the case experimentally (see p. 17, Chapter II-D-3).

V. CONCLUSIONS

A. Experimental Contributions

Four specific contributions to the field of experimental photoconductivity and surface physics were made:

1. A beat frequency bridge method was conceived and developed for field effect studies which allows for an accurate determination of field effect time constant, the combined trapping efficiency of the surface and space charge states, and the effective mobility.

2. The identity of the field effect and photoconductive time constants, independent of background illumination, film surface condition, and side of film probed, was established for chemically deposited PbS films.

3. Field effect mobility was determined to be equal to the Hall mobility.

4. One insensitive film was also studied. The results indicated no clear field effect time constant and that $\alpha \cong 0$.

B. Theoretical Contributions

1. The majority carrier model was extended so as to describe field effect measurements by including explicitly the time constants for charge transfer into and out of the majority carrier traps.

2. Equations were developed for estimating the densities and capture cross-sections of the majority carrier traps. These equations demonstrate the usefulness of field effect in further identifying the fundamental mechanism of photoconductivity in thin films.

3. An analysis was made of homogeneous polycrystalline films for crystallite dimensions both larger and smaller than a Debye length. The analysis yields both photoresponse and field effect time constants in terms of the time constants which characterize the bulk, space charge, and surface state trapping.

C. Summary of Conclusions

Interpretation of the experimental data with due consideration of the theory developed yields the following principal conclusions concerning the PbS films studied:

1. The majority carrier lifetime is predominant in the photoconductive process.

2. The rate limiting process in a sensitized film is the rate of transfer of charge into the traps.

3. The density of majority carrier traps is high while the capture-cross-section is very small, conditions required for the long majority time constants measured. The estimated density of surface traps required to provide the time constants measured is of the order expected on crystallites with dimensions of the order of 0.1 microns. The density of bulk traps estimated to provide the time constants is larger than would be expected.

4. The film is a homogeneous polycrystalline structure composed of crystallites

with dimensions of the order of a Debye length or less.

5. The traps probed by field effect measurements are a representative sample of those which cause photoconductivity. Field effect measurements will provide a useful tool for the further clarification of the mechanism of photoconductivity in thin films, and its relation to the sensitization process.

D. Recommendations for Future Research

1. Additional surface state studies should be made on sensitive film to further determine the effective density, energy relative to the main bands, and effective cross-sectional area of the traps. This pertinent information should be obtainable from a series of measurements of the time constant and α as a function of temperature and ambients.

2. Surface studies should be made on a series of films covering a range of sensitivity along with other fundamental measurements of sensitivity, time constant, responsitivity and noise. The measurement of α and τ_f offer a direct means of evaluating the density and cross-section of the photoconductive traps. Such measurements, when correlated with the sensitization conditions should lead to an improved understanding of the sensitization process.

3. A series of precision absolute field effect measurements should be made to determine accurately the extent of barrier modulation and the space charge region mobility.

ACKNOWLEDGMENTS

Catholic University of America kindly permitted the research reported herein to be performed off campus under a program jointly sponsored by the Naval Ordnance Laboratory, White Oak, Maryland and the Office of Naval Research, Washington, D. C. The sincere interest of the Navy in science is shown by the policy of ONR which encourages its scientific administrators to perform basic research studies. In particular, I wish to thank Drs. Robertson, Silverman, and Shostak of ONR for their personal interest and encouragement. I am indebted to the NOL for space, facilities and the opportunity of performing research under their Foundational Research Funds. Discussions with Drs. Jay N. Zemel, James N. Humphrey, Joseph F. Woods, and Miss Frances L. Lummis concerning both the theory and apparatus were beneficial. Suggestions concerning both the analysis of data and organization of the report by readers Drs. F. T. Byrne and Jay N. Zemel contributed much to the report. Finally, the guidance and contributions of Dr. Richard L. Petritz, the Major Professor, were invaluable.

APPENDIX

1. Balanced Bridge Equations

Refer to Fig. 29 for nomenclature and assume that either the FE or a light pulse causes a change ΔR in the resistance R of the film. The resulting voltage change ΔV_o across the film terminals is then

$$\Delta V_o = I_s \Delta R + R \Delta I_s \ , \qquad \text{(A-1,1)}$$

where I_s is the dc current through the film and ΔI_s is the change in current in the film produced by ΔR. The equation for I_s is

$$I_s = V_b / (R_1 + R_2 + R) \ , \qquad \text{(A-1,2)}$$

and $$\Delta I_s = \frac{-V_b \Delta R}{(R_1 + R_2 + R)(R_1 + R_2 + R + \Delta R)} \ , \qquad \text{(A-1,3)}$$

where V_b is the bias provided by a stabilized voltage, i.e. low impedance source. We may now write:

$$\Delta V_o = I_s \Delta R \left(\frac{R_1 + R_2 + \Delta R}{R_1 + R_2 + R + \Delta R} \right) . \qquad \text{(A-1,4)}$$

In this particular bridge $R_1 = R_2 = 10k$ ohms, $R \sim 1000k$ ohms, and $\Delta R < 4k$ ohms even for the maximum resistance change; therefore

$\Delta R << R_1 + R_2 + R$ and $\Delta R < R_1 + R_2$. In the following we consider terms to ΔR, and neglect terms of order ΔR^2 and higher. The voltage across the output terminals of the bridge as measured with an infinite impedance detector is then

$$\Delta V_o = I_s \Delta R \left(\frac{R_1 + R_2}{R_1 + R_2 + R} \right) . \qquad \text{(A-1,5)}$$

Since $R = \frac{1}{G}$ and $\Delta R = \frac{-1}{G^2} \Delta G = -\Delta G \, R^2$, Eq. (A-1,5) can be written as

$$\Delta V_o = -I_s \Delta G \, R^2 \left(\frac{R_1 + R_2}{R_1 + R_2 + R} \right) . \qquad \text{(A-1,6)}$$

From the equivalent circuit (Fig. 30) for Eq. (A1, 5), one sees that ΔR causes an open-circuit voltage V_{oc} across the film terminals. The film is loaded with R_1 and R_2 in series which decreases the voltage output to V_o. This equivalent circuit is useful for estimating the effect of a loading of the detector by a differential amplifier with an input resistance R_d of 10 megohms. The total input capacity C_d including the amplifier, the lead capacity, and the self-capacitance of the film, was of the order of 50 micro-micro Farads. The RC time constant for the equivalent bridge circuit is

$$\tau_{RC} = \frac{(R_1 + R_2) R}{R_1 + R_2 + R} C_d \ .$$

For the values of R_1, R_2, R, and C_d used, $\tau_{RC} \sim 1$ microsec. The measured FE and photoresponse time τ_f and τ_p were longer than 100 microsec, so that the capacitance loading of the detector was negligible.

Defining a quantity F_f as

$$F_f = \frac{\Delta R}{R}\frac{1}{V_f} = -\frac{\Delta G R}{V_f}\,, \qquad \text{(A-1,7)}$$

which is the fractional change in resistance per field effect volt. An equation relating the field effect voltage to ΔV_o can be obtained by substituting Eq. (A-1,7) into Eq. (A-1,5), so that

$$\Delta V_o = I_s F_f R V_f \left(\frac{R_1 + R_2}{R_1 + R_2 + R}\right)\,, \qquad \text{(A-1,8)}$$

where F_f is a function of time.

2. Beat-Frequency Bridge Equations

At the beginning of each measurement of field effect or photoresponse with the beat-frequency bridge shown schematically in Fig. 31, the bridge was balanced at the bridge bias supply frequency b by adjusting R and C for minimum signal on the wave analyzer when tuned to b. At balance, the resistance R and capacitance C of the bridge were equal to the resistance and self capacity respectively of the PbS film sample. When either a sinusoidal voltage of frequency f was applied to the field effect plate or a pulsed light of frequency f was incident on the film, the bridge was not unbalanced at frequency b; however, a voltage $V_{(w)}$ was observed when the wave analyzer was tuned to either (f + b) or (f - b). The purpose of this Appendix is to relate $V_{(w)}$ to the field effect and photoresponse of the film.

Conventional balanced bridge type equations are not used in this analysis as the bridge was balanced only for the purpose of preventing the bias supply voltage from saturating the

wave analyzer. The phenomenon of interest is the modulation of the film resistance at the field effect or light signal frequency f. The time dependent incremental modulation ΔR_f of the film resistance R by the field effect is

$$\Delta R_f = -F_f R V_f \sin 2\pi f t\,, \qquad \text{(A-2,1)}$$

where F_f is defined as the fractional change in film resistance at the field effect frequency per field effect volt. An ac change in the film resistance arises due to the bridge bias voltage which changed the film potential relative to the field effect plate at frequency b. This resistance change is

$$\Delta R_b = \tfrac{1}{2} F_b R V_b \sin 2\pi b t\,, \qquad \text{(A-2,2)}$$

where F_b is the fractional change in film resistance at the bias frequency per bias volt. F_b is divided by 2 because the voltage between the field effect plate and the film increases linearly along the film from 0 to V_b.

$\Delta R/R$ per field effect volt was shown experimentally to be independent of the bias and field effect voltages (see Fig. 32). ΔR is interpreted as a linear function of the field effect voltage. Because of this linearity and the ohmic nature of the film as shown in Fig. 33, the principle of superposition was used to predict the total $\Delta R/R$ in terms of V_b and V_f. The resulting equation is

$$\frac{\Delta R}{R} = -F_f V_f \sin 2\pi f t + \tfrac{1}{2} F_b V_b \sin 2\pi b t. \qquad \text{(A-2,3)}$$

The relative phases of the field effect voltage and the bias voltage sources at t=0 are not considered since the sources are not synchronized.

The instantaneous open-circuit resistance of the film in response to the field effect and bias voltages is

$$R_{oc} = R\left(1 + \frac{\Delta R}{R}\right). \qquad \text{(A-2,4)}$$

The current I_s through the film as a result of the bias voltage V_b is

$$I_s = V_b \sin 2\pi bt. \qquad \text{(A-2,5)}$$

From Eqs. (A-2,3), (A-2,4) and (A-2,5), the equation for the open-circuit voltage V_{oc} across the film terminals is

$$V_{oc} = I_s R_{oc}$$
$$= V_b \sin 2\pi bt \left(1 - F_f V_f \sin 2\pi ft + \tfrac{1}{2} F_b V_b \sin 2\pi bt\right). \qquad \text{(A-2,6)}$$

Using the trigonometric identity

$$\sin x \sin y = \tfrac{1}{2}\left[\cos(x-y) - \cos(x+y)\right],$$

$$V_{oc} = V_b \sin 2\pi bt$$
$$- F_f V_b V_f \left[\cos 2\pi(f-b)t - \cos 2\pi(f+b)t\right] \qquad \text{(A-2,7)}$$
$$+ \tfrac{1}{4} F_b V_b^2 \left[1 - \cos(2\pi 2bt)\right].$$

Equation (A-2,7) states that the open-circuit voltage across the film terminals is the superposition of the bias voltage at b, sine wave voltages at sum (f + b) and difference

(f - b) frequencies, a dc voltage, and a voltage whose frequency is 2b. There are no cross modulation terms, i.e. F and F_b are independent. The possibility of cross modulation was eliminated in the derivation when linear modulation was assumed. There is considerable latitude in selecting the specific voltage component to be measured in the field effect measurements. Field effect could be determined from a measurement of either the dc, second harmonic 2b, sum (f + b) or difference (f - b) frequency components of V_{oc}. Those measurements involving the second harmonic require bridge bias sources with low harmonic content, particularly low second harmonic. Field effect measurements which involve the dc components of V_{oc} usually are made by placing a dc current meter in series with the bridge.[33] The current meter must be capable of precise measurement of quite small currents. In this experiment the sum and/or difference frequency components $V_{(f \pm b)}$ were measured with a wave analyzer.

From Eq. (A-2,7) the magnitude of F_f in terms of the rms values of V_b, V_f, and $V_{(f \pm b)}$ is

$$F_f = \frac{\sqrt{2}\, V_{(f \pm b)}}{V_b V_f}. \qquad \text{(A-2,8)}$$

The open-circuit voltage $V_{(f \pm b)}$ was not measured directly. The film terminals, across which the open-circuit voltage was calculated, were loaded with the self-capacity of the film due to the field effect plate, the resistance R, the capacitance C, the capacitance C_ℓ of the leads from the bridge to the wave analyzer, the input impedance Z_w of the wave analyzer, and the resistance $R_t/2$ of the bias transformer T. According to Thevinen's theorem, the circuit in Fig. 34 may be equated to the beat-frequency bridge of Fig. 31 to determine the relation

between $V_{(f \pm b)}$ and $V_{(w)}$. All of the elements of the equivalent circuit Fig. 34 could have been measured individually and the relationship between $V_{(f \pm b)}$ and $V_{(w)}$ then obtained by direct but tedious circuit calculations. A more practical procedure was to insert a relatively low-impedance generator of known frequency and voltage in the place of $V_{(f \pm b)}$, i.e. in series with the PbS film, and note the ratio (known voltage / $V_{(w)}$) which is L_w. The known voltage was inserted in series with the film by changing the positions of switches 1 and 2, (see Fig. 31) from a to b.

Because of the high impedance of the film and the wave analyzer input, capacity loading caused the ratio L_w to be frequency dependent as shown in Fig. 10. L_w is plotted for selected values of background illumination intensity stated in terms of light bias voltage.

Having experimentally determined L_w, Eq. (A-2,8) can be modified to present F_f in terms of measurable parameters including $V_{(w)}$:

$$F_f = \frac{\sqrt{2}\, L\, V_{(w)}}{V_b V_f} . \qquad \text{(A-2,9)}$$

The field effect voltage is at frequency f; however, $V_{(w)}$ is the voltage indicated by the wave analyzer which is tuned to either (f + b) or (f - b). Because of the frequency dispersion, the value of L_w selected must correspond to the frequency (f + b) or (f - b) to which the wave analyzer is tuned.

In the case of the photo-response measurements using the beat-frequency bridge, the pulsed light incident on the PbS film modulates the film resistance R by an amount ΔR at the pulse repetition rate f. The fundamental component of ΔR beats with bias voltage V_b at frequency

b to provide open-circuit voltages $V_{(f \pm b)}$ and $V_{(f - b)}$ and in turn $V_{(w)}$ was measured with the wave analyzer. Of course, the higher harmonics of ΔR beat with the bias voltage to provide signals at the bias plus or minus the harmonic frequency. These harmonic components of the bridge output were rejected by the wave analyzer which measured $V_{(f \pm b)}$ just as in the field effect measurements. From (A1,9) and (A-2,9 the fractional change in the film resistance ΔR / R due to the incident light signal is

$$\frac{\Delta R}{R} = \frac{\sqrt{2}\, L_w V_{(w)}}{V_b} \qquad \text{(A-2,10)}$$

an equation which holds independent of what causes the ΔR at the frequency or pulse repetition rate f.

3. Check on Ohmic Nature Of PbS Photosensitive Films

The ohmic nature of the film resistance was determined by a series of dc current versus voltage measurements at selected values of background illumination intensity. Figure 33 shows the film to be ohmic within the accuracy of measurement.

4. Exploratory Measurements Using Balanced Bridge

The circuitry of the FE plate was modified to permit the application of large (up to 105 volts per cm) dc electric fields transverse to the film surface during FE and photoresponse measurements. For a brief period, often as long as a minute, immediately following the application of the dc field spurious electrical tran-

sients prevented measurements. After this period, the response to both light and FE differed by as much as 10% from the response with no dc fields. Within several minutes, this change in sensitivity gradually decreased to zero. The sensitivity decreased when the dc potential of the plate was made negative and increased when it was made positive. This phenomenon is believed to be due to the filling of the slow or outer states on the surface. When the dc potential was negative majority carriers, in this case holes, were induced into the bulk which caused a decrease in resistance. As time progressed, first the fast surface states came to equilibrium, then the slow states, until finally the bulk was partially shielded from the dc field. Presumably, there was an insufficient density of induced surface charge to substantially change the time constants associated with net transfer of charge between the bulk and fast states. This assumption is substantiated by the fact that neither the amplitudes nor time constants of the field effect or photoresponse were appreciably altered by the presence of the dc electrostatic field.

In a somewhat similar experiment on a number of different films, attempts to invert the space charge layer by the application of large dc and 60 cps voltages on the FE plate were not successful. The amplitude of field effect voltages were increased until the oscilloscope monitor of the bridge response indicated considerable bursts of noise as might be expected for weak breakdown or arcing. The fact that a surface inversion layer could not be induced is further confirmation that dc or show ac fields do not substantially alter the properties of the film interface.

On one film, the space charge region properties were altered by background illumina-

tion in a unique manner. As shown in Fig. 35a, the response for no background illumination was a maximum at the initiation of a FE voltage pulse and then decayed to a quasi-equilibrium value. However, if the background illumination was sufficiently large, the response was not a maximum immediately following the FE pulse but increased in a somewhat non-exponental fashion to an equilibrium value. These particular experiments were repeated using ac FE voltages over a range of frequencies with with approximately the same results. No interpretation is attempted.

BIBLIOGRAPHY

1. R. L. Petritz, Physical Review, 104, 1508 (1956).

2. E. S. Rittner, in Photoconductivity Conference, edited by Breckenridge, Russell and Hahn (John Wiley and Sons, Inc., New York 1956) 215.

3. Albert Rose, Proceedings of the Institute of Radio Engineers, 43, 1850 (1955).

4. T. S. Moss, Proc. IRE, 43, 1869 (1955).

5. R. A. Smith, Advances in Physics, Vol. 2, 321 (1953).

6. H. Pick, Z. Physik, 126, 12 (1949); Doughty, Lark-Horovitz, Roth, and Shapiro, Physical Review 79, 203A (1950); H. T. Minden, J. Chem. Physics 23, 1948 (1955).

7. R. F. Brebrick and W. W. Scanlon, Phys. Rev. 96, 598, (1954).

8. W. Smith, American Journal of Science, 5, 301, (1873).

9. T. W. Case, Phys. Rev., 9, 305 (1917).

10. R. L. Petritz and J. N. Humphrey, "Research on Photoconductive Films of the Lead Salt at U. S. Naval Ordnance Laboratory, White Oak, Md." (To be published by IRIS) also NAVORD 6042.

11. J. N. Humphrey and R. L. Petritz, Phys. Rev., 105, 1736 (1957).

12. W. W. Scanlon, Phys. Rev., 92, 1573 (1953).

13. R. P. Chasmar in Photoconductivity Conference, edited by Breckenridge, Russell and Hahn. (John Wiley and Sons, Inc., N. Y. and Chapman and Hall, Lmtd., London 1956) p. 463.
R. A. Smith, Physica 20, 990 (1954).

14. A von Hipple and E. S. Rittner, J. Chem. Physics, 14, 370 (1946).

15. J. C. Slater, Phys. Rev., 103, 1631 (1956).

16. Mahlman, Nottingham and Slater, in Photoconductivity Conference, (John Wiley and Sons, Inc., New York and Chapman and Hall, Lmtd., London 1956) 469, edited by Breckenridge, Russell and Hahn.

17. F. L. Lummis and R. L. Petritz, Phys. Rev., 105, 502 (1957).

18. R. L. Petritz and F. L. Lummis (to be published).

19. J. F. Woods, Phys. Rev., 106, 235 (1957).

20. A. Rose, Phys. Rev., 97, 322 (1955).

21. J. N. Humphrey and W. W. Scanlon, Phys. Rev., 105, 469 (1957).

22. R. L. Petritz, Bull. Am. Phys. Soc., Ser II, 1, 177T(1956).

23. R. H. Kingston, J. of Applied Physics, 27, 101 (1956).

24. Semiconductor Surface Physics, edited by R. H. Kingston (Univ. of Penn. Press, Phila., Penn. 1957).

25. I. Tamm, Physik Z. Sowjetumion, I, 733 (1932).

26. W. Shockley, Phys. Rev., 56, 317 (1939).

27. J. Bardeen, Phys. Rev., 71, 717 (1947).

28. J. Zemel, in Semiconductor Surface Physics, edited by R. H. Kingston, (Univ. of Penn. Press, Phila., Penn. 1957) 193.

29. H. Rzewoski and L. Sosnowski, Bulletin De L'Academic Polonaise Des Sciences Classe Troisieme, II, Numero 2, Varsovie 1955.

30. H. E. Sorrows, Bull. Am. Phys. Soc., Ser. II, 2, 131 (1957).

31. Petritz, Lummis, Sorrows and Woods, in Semiconductor Surface Physics, edited by R. H. Kingston (Univ. of Penn. Press, Phila., Penn. 1957) 229.

32. C. G. B. Garrett, Phys. Rev., 107, 478 (1957).

33. H. C. Montgomery, Phys. Rev., 106, 441 (1957).

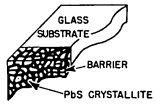

FIG. 1 ENVISAGED MICROSCOPIC STRUCTURE OF PbS THIN FILM PHOTOSENSITIVE SAMPLES

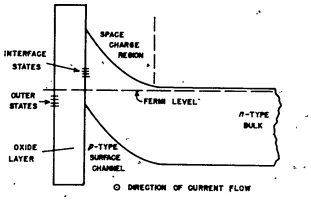

FIG. 2 TYPICAL SEMICONDUCTOR SURFACE

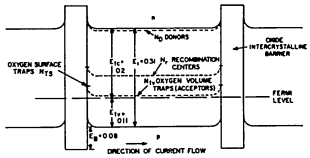

FIG. 3 ENERGY LEVELS IN A PbS PHOTOCONDUCTIVE FILM

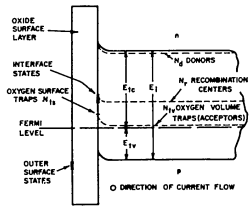

FIG. 4 OUTER SURFACE OF A PbS FILM

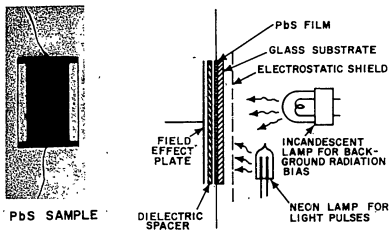

FIG. 5 COMPONENTS FOR PHOTO RESPONSE AND FIELD EFFECT MEASUREMENTS

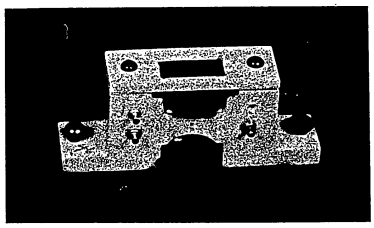

FIG. 6A ASSEMBLED SAMPLE HOLDER

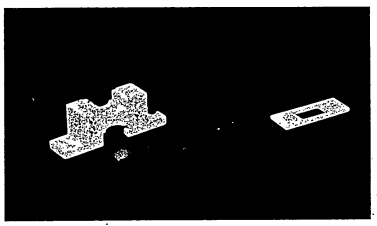

FIG. 6B DISMANTLED SAMPLE HOLDER

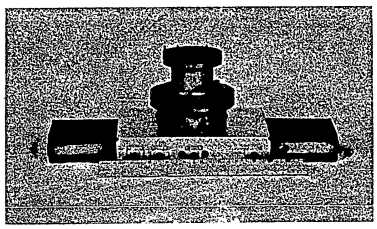

FIG. 7A ASSEMBLED SAMPLE HOUSING

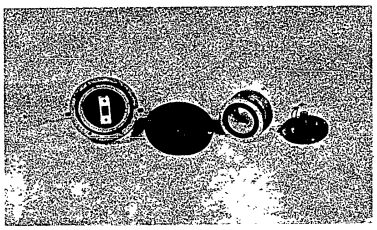

FIG. 7B DISMANTLED SAMPLE HOUSING

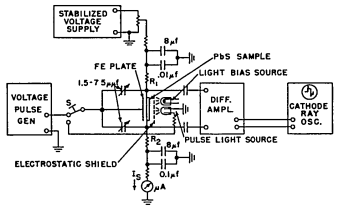

FIG 8 BALANCED BRIDGE SETUP

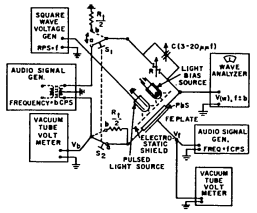

FIG. 9 BEAT FREQUENCY BRIDGE SETUP

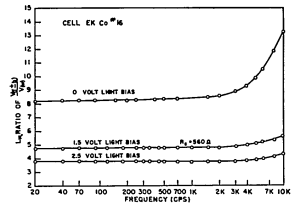

FIG. 10 EXAMPLE OF CALIBRATION OF BEAT-FREQUENCY BRIDGE SETUP

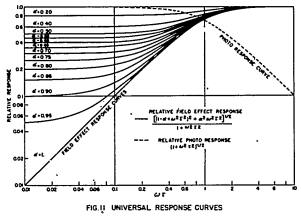

FIG. 11 UNIVERSAL RESPONSE CURVES

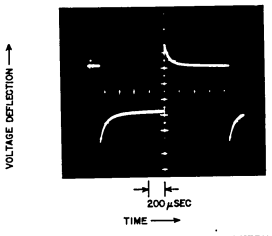

FIG. 12 TYPICAL OSCILLOSCOPE PATTERN OF RESPONSE TO SQUARE WAVE FIELD EFFECT VOLTAGE

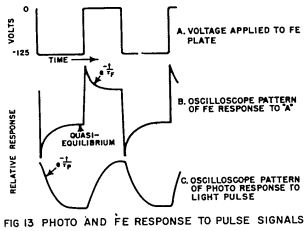

FIG 13 PHOTO AND FE RESPONSE TO PULSE SIGNALS

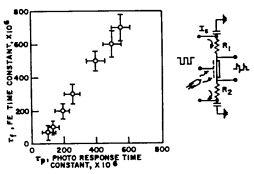

FIG. 14 BALANCED BRIDGE DATA ON TIME CONSTANTS

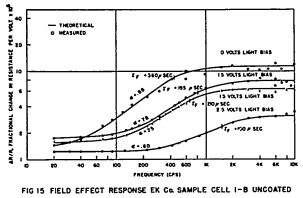

FIG 15 FIELD EFFECT RESPONSE EK Co. SAMPLE CELL I-B UNCOATED

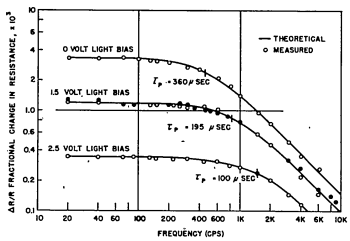

FIG.16 PHOTOCONDUCTIVE RESPONSE, EK Co CELL I-B UNCOATED

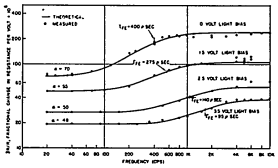

FIG.17 FIELD EFFECT RESPONSE EK Co CELL I-A PLASTIC COATED

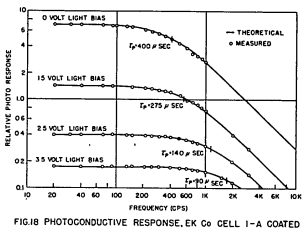

FIG.18 PHOTOCONDUCTIVE RESPONSE, EK Co CELL I-A COATED

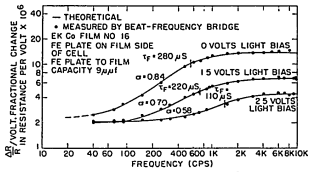

FIG 19 FIELD EFFECT RESPONSE OF UNCOATED FILM

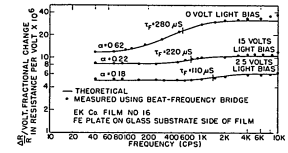

FIG 20 FIELD EFFECT RESPONSE OF GLASS SUBSTRATE SURFACE

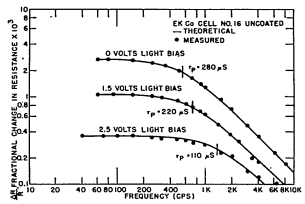

FIG.21 PHOTO RESPONSE TIME VS BACKGROUND ILLUMINATION

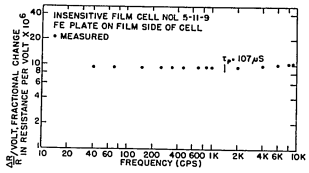

FIG 22 FIELD EFFECT RESPONSE FOR INSENSITIVE FILM

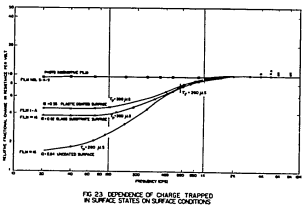

FIG 23 DEPENDENCE OF CHARGE TRAPPED IN SURFACE STATES ON SURFACE CONDITIONS

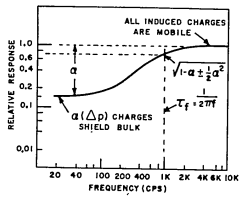

FIG. 24 TYPICAL RELATIVE RESPONSE TO A SINUSOIDAL FIELD-EFFECT VOLTAGE

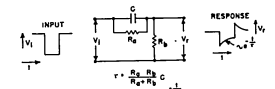

FOR A STEP FUNCTION V_i : $V_r = V_i\left(\frac{R_b + R_a e^{-\frac{t}{\tau}}}{R_b+R_a}\right)$

FOR A SINUSOIDAL V_i: $V_r = V_i \sqrt{\frac{\left(\frac{R_b}{R_a+R_b} + \tau^2\omega^2\right)^2 + \left(\frac{R_a\omega\tau}{R_a+R_b}\right)^2}{1+\tau^2\omega^2}}$, θ

WHERE $\theta = \tan^{-1}\left[\frac{R_a\omega\tau}{(R_a+R_b)\omega^2\tau^2+R_b}\right]$

FIG.25 RC ANALOGUE OF FE RESPONSE

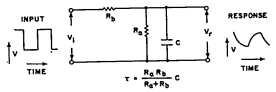

FOR A STEP FUNCTION V_i : $V_r = V_i\left[\frac{R_a}{R_a+R_b}(1-e^{-\frac{t}{\tau}})\right]$

FOR A SINUSOIDAL V_i : $V_r = V_i \left[\frac{R_a}{R_a+R_b}\sqrt{\frac{1}{1+\frac{R_a^2 R_b^2}{(R_a+R_b)^2}\omega^2 C^2}}\right]$, θ

$\theta = \tan^{-1}\left(\frac{R_a R_b \omega C}{R_a+R_b}\right)$

FIG.26 RC ANALOGUE OF PHOTO RESPONSE

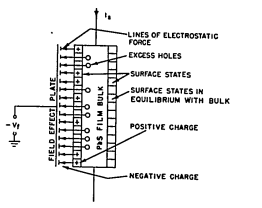

FIG.27 PICTORIAL REPRESENTATION OF ROLE OF ELECTRONIC SURFACE STATES IN FIELD EFFECT EXPERIMENTS

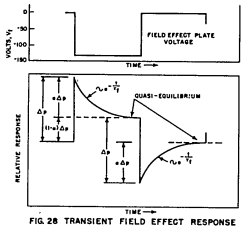

FIG. 28 TRANSIENT FIELD EFFECT RESPONSE

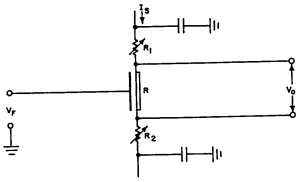

FIG. 29 SIMPLIFIED BALANCE BRIDGE CIRCUIT

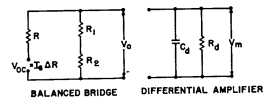

FIG 30 EQUIVALENT CIRCUIT FOR BALANCED BRIDGE WITH DIFFERENTIAL AMPLIFIER LOADING

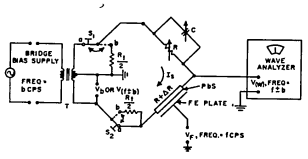

FIG. 31 CIRCUIT FOR FIELD EFFECT AND PHOTO-CONDUCTIVE RESPONSE MEASUREMENTS WITH BEAT FREQUENCY BRIDGE

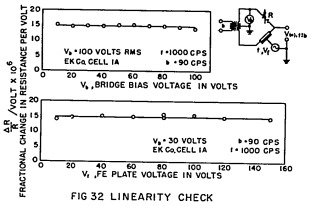

FIG 32 LINEARITY CHECK

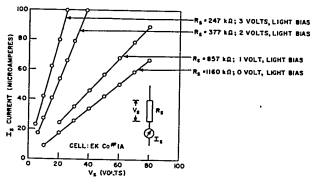

FIG. 33 CHECK OF OHMIC PROPERTY

STAT

Next 9 Page(s) In Document Denied